UNCLASSIFIED

AD NUMBER
AD820738
LIMITATION CHANGES

TO:

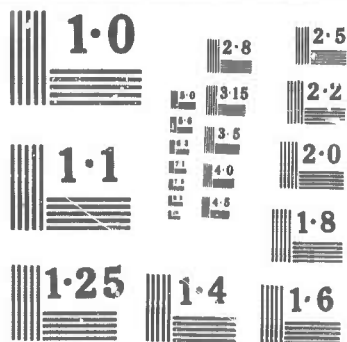Approved for public release; distribution is unlimited.

FROM:

Distribution authorized to U.S. Gov't. agencies and their contractors; Critical Technology; SEP 1967. Other requests shall be referred to Air Force Technical Applications Center, Washington, DC 20333. This document contains export-controlled technical data.

AUTHORITY

usaf ltr, 25 jan 1972

THIS PAGE IS UNCLASSIFIED

AD820738

LARGE-ARRAY SIGNAL AND NOISE ANALYSIS

Special Scientific Report No. 5

DETECTION OF DISCRETE ARRIVALS
IN MANTLE P-WAVE NOISE

Prepared by
Donald B. Crouch

Frank H. Binder, Program Manager

TEXAS INSTRUMENTS INCORPORATED
Science Services Division
P. O. Box 5621
Dallas, Texas 75222

Prepared for

AIR FORCE TECHNICAL APPLICATIONS CENTER
Washington, D.C. 20333

Sponsored by

ADVANCED RESEARCH PROJECTS AGENCY
ARPA Order No. 599
AFTAC Project No. VT/6707

6 September 1967

LARC -ARRAY SIGNAL AND NOISE ANALYSIS

Special Scientific Report No. 5

DETECTION OF DISCRETE ARRIVALS
IN MANTLE P-WAVE NOISE

Prepared by
Donald B. Crouch

Frank H. Binder, Program Manager

TEXAS INSTRUMENTS INCORPORATED
Science Services Division
P. O. Box 5621
Dallas, Texas 75222

ABSTRACT

An exponential relation, $\log N = a - bM$ where N is the annual number of earthquakes of magnitude M, is generally accepted to exist between the number of earthquakes occurring in a given time and the earthquake magnitude. A linear least-squares solution of this equation indicates that a small earthquake ($2 < M < 3$) occurs every 30 sec. The only difference between these small P waves and an event is one of magnitude; therefore, it is reasonable to expect that the P-wave noise would contain discrete P-wave arrivals which travel across the array as plane waves. The purpose of this study is to identify and describe (statistically) such discrete arrivals.

Two techniques have been used to identify discrete arrivals. One method, Fisher analysis of variance, provides an output time function which measures the likelihood of an arrival in a specific segment of noise. The other technique calculates a moving power spectra and looks for spectral characteristics which are sufficiently deviant from the expected values of a Gaussian stationary process. Using an 8-min noise sample, the methods were able to detect no discrete arrivals propagating across the array like plane waves. Within the resolving power of these tests, no small P wavelets appeared to be in the mantle P-wave noise

TABLE OF CONTENTS

LIST OF APPENDIXES

LIST OF ILLUSTRATIONS

LIST OF ILLUSTRATIONS (CONTD)

TABLE

SECTION I
INTRODUCTION AND SUMMARY

This report presents results of an investigation of discrete arrivals in mantle P-wave noise.

An exponential relation is generally accepted to exist between the number of earthquakes occurring in a given time and the earthquake magnitude. Richter [1] gives this relation as $\log N = a - bM$ where N is the annual number of earthquakes of magnitude M. A linear least-squares solution of this equation, developed from data of 1960 and 1963,[2] indicates that a small earthquake $(2 < M < 3)$ occurs every 30 sec. The only difference between these small P waves and an event is one of magnitude; therefore, it is reasonable to expect that the P-wave noise would contain discrete P-wave arrivals which travel across the array as plane waves. The purpose of this study is to identify and describe (statistically) such discrete arrivals.

Two techniques have been used to identify discrete arrivals. One method, Fisher analysis of variance, provides an output time function which measures the likelihood of an arrival in a specific segment of noise. The other technique calculates a moving power spectra and looks for spectral characteristics which are sufficiently deviant from the expected values of a Gaussian stationary process. Theoretical discussions of these methods and derivations of formulas are included in Section II.

Using an 8-min noise sample, the methods were able to detect no discrete arrivals propagating across the array like plane waves. Within the resolving power of the above tests (discussed in Section III), no small P wavelets appeared to be in the mantle P-wave noise.

SECTION II
METHODS OF DETECTION

A. FISHER ANALYSIS OF VARIANCE

The analysis-of-variance technique is a method of signal detection applicable only to array data. This method depends on the similarity of signals across channels as compared to the noise. The basic computation provides an output function of time, each point of which can be translated into a probability that a specific segment of the original array data contains a signal. This technique has been developed in previous literature,[3] but a brief discussion of the theory is presented here for the reader's convenience.

The mathematical model for array data which has been developed is

$$X_{ij} = \mu + t_j + \epsilon_{ij}$$

for $i = 1, \ldots, r$ and $j = 1, \ldots, s$ where the parameters have the following meaning:

X_{ij} is the observed value for i^{th} channel, j^{th} time

ϵ_{ij} is random noise

μ is overall mean (expected to be 0)

t_j is signal effect, alike across instruments in a given subarray but different in time and for different subarrays

The noise term ϵ_{ij} is assumed to be normally and independently distributed around a mean of 0 with an unknown but constant variance σ^2. Thus, the distribution function of any single observation X_{ij} may be written

$$f(x_{ij}) = \frac{1}{\sigma\sqrt{2\pi}} \exp - 1/2 \frac{\left[X_{ij} - \mu - t_j\right]^2}{\sigma^2}$$

and, from the assumption of independence, the joint distribution of all observations is

$$f = \prod_{i,j} f(x_{ij})$$

With these assumptions, it is possible to derive a criterion (Fisher's F) to test the hypothesis

$$Ho: t_j = 0$$

for $j = 1, \ldots, s$. It can be shown that F is equivalent to a likelihood ratio test λ of the hypothesis that there is no similar signal effect, as compared to the noise, across r instruments within corresponding noise segments of time-width s. The likelihood ratio test of Ho is defined as

$$\lambda = \frac{\max\limits_{\mu,\sigma^2}\left[\prod\limits_{i,j} f(x_{ij}; \mu, \sigma^2, t = 0)\right]}{\max\limits_{\mu,\sigma^2,t}\left[\prod\limits_{i,j} f(x_{ij}; \mu, \sigma^2, t_j)\right]}$$

where max [L] is the greatest value that the likelihood function L can assume. It is clear that λ tends to be less when the t_j's are nonzero than when the t_j's are zero, since the likelihood function in the numerator cannot exceed the likelihood function in the denominator. Thus, λ cannot exceed 1 and is always positive. Therefore, it is reasonable to reject the hypothesis Ho when λ is less than or equal to some critical value λc; i.e., the values of λ for which Ho would be rejected satisfy $0 \leq \lambda \leq \lambda c$.

It has been shown that λ and F are related by a monotone function in such a manner that large values of F correspond to small values of λ; thus, the critical region for the Fisher values is the interval $Fc \leq F \leq \infty$ where Fc is the critical value of F. A signal is considered present in the noise if $F > Fc$, and no signal is present if $F \leq Fc$. Tables of the distribution of F are readily available, and Fc can be easily obtained from the desired false-alarm rate.

B. DYNAMIC POWER SPECTRA

The dynamic-power-spectra method calculates a moving power spectra and looks for anomalously high power in a given frequency band. The purpose is to detect discrete arrivals by looking for spectral characteristics which are sufficiently deviant from the expected values of a Gaussian stationary process.

Consider a time trace of length T, sampled at a rate Δt, having NP points. This trace is divided into 64-point overlapping blocks so that the 33rd point of one block corresponds to the first point of the subsequent block. The complex Fourier transform of each block is taken, using the Cooley-Tukey algorithm.[4] Multiplying the Fourier transform by its complex conjugate yields the measured power spectra of the 64-point data block. The first 32 positive frequencies are retained, from 0 to $f_{max} - \Delta f$, in equal steps of Δf where

$$\Delta f = \frac{1}{64\Delta t}$$

and

$$f_{max} = \frac{1}{2\Delta t}$$

The average measured power spectrum of the trace is found by averaging the measured power spectra values at a given frequency for all the nonoverlapping but adjacent data blocks, i.e., averaging the values at a given frequency from the first, third, fifth, etc., data blocks. The measured power spectra of the data blocks are smoothed over two frequencies and decimated, yielding a power spectrum having 16 frequency points. This method is very similar to one previously published by Haubrich.[5]

A significantly different behavior from the average at some range in the time trace may be determined by noting if the power spectrum of some data block is higher than the average over some band of frequencies.

This behavior is called signal. The signal may be characterized by a vector in a p-dimensional space, each dimension corresponding to a frequency and having components

$$\frac{Z_i - N_i}{\sigma_i}$$

at the ith frequency where Z_i is the measured power spectrum (smoothed or unsmoothed), N_i is the average, and σ_i is the standard deviation. The magnitude of the vector M is then

$$M = \sqrt{\sum_{i=1}^{p} \left(\frac{Z_i - N_i}{\sigma_i}\right)^2}$$

where p is the number of dimensions. Explicit expressions for N_i and σ_i are given by

$$N_i = \frac{1}{MB} \sum_{j=1}^{MB} Z_{ij}$$

and

$$\sigma_i = \sqrt{\sum_{j=1}^{MB} \left(\frac{Z_{ij} - N_i}{MB - 1}\right)^2}$$

where Z_{ij} is the measured power spectrum of the jth data block at the ith frequency and MB is the number of nonoverlapping data blocks.

As shown in Appendix A, assuming that the time trace is the output of a Gaussian process, the measured (unsmoothed) power spectrum is distributed as a constant times a χ^2 function having two degrees of freedom, and the frequency points (as calculated above) are independent. The average measured power spectrum is taken to approximate the true power spectrum.

This approximation simplifies the theoretical work; thus, smoothing over two frequency points corresponds to a χ^2 distribution with four degrees of freedom.

Based on experiments with traces of Gaussian random noise (autocorrelated), the decision was made to try two different techniques of smoothing and analyzing the data. One consists of averaging the adjacent frequencies, decimating to 16 frequency points, and looking at a vector formed by three adjacent smoothed frequencies (i.e., six original frequency increments). Only blocks having smoothed spectral estimates which are higher than the average (N_i) at all three frequencies are considered significant. The magnitude of the resulting 3-dimensional vector (M) is then examined to give greater discrimination. The second method would be identical to the first except that four adjacent smoothed frequencies (eight original frequency increments) are used.

Using these theoretical distributions of the spectral estimates, a false-alarm rate is established for two types of analysis; i.e., a probability number that a 64-point block yield a frequency-domain vector of given magnitude with each component larger than the average spectrum (N_i) is assigned to the events. The details of this derivation, which involve a simplifying assumption, are given in Appendix B. The results are shown in Figures II-1 and II-2.

Figure II-1 plots the probability of occurrence against the magnitude of the 3-dimensional vector. This probability graph assumes that all of the three components exceed the estimated true spectrum N_i.

Figure II-2 plots the probability of occurrence vs magnitude of the 4-dimensional vector. This probability graph assumes that all of the four components exceed N_i.

To verify the reliability of the dynamic-power-spectra technique as a method of signal detection, 12 traces of autocorrelated Gaussian noise which are 4000 points in length and have a sampling rate of 0.1 sec are generated.
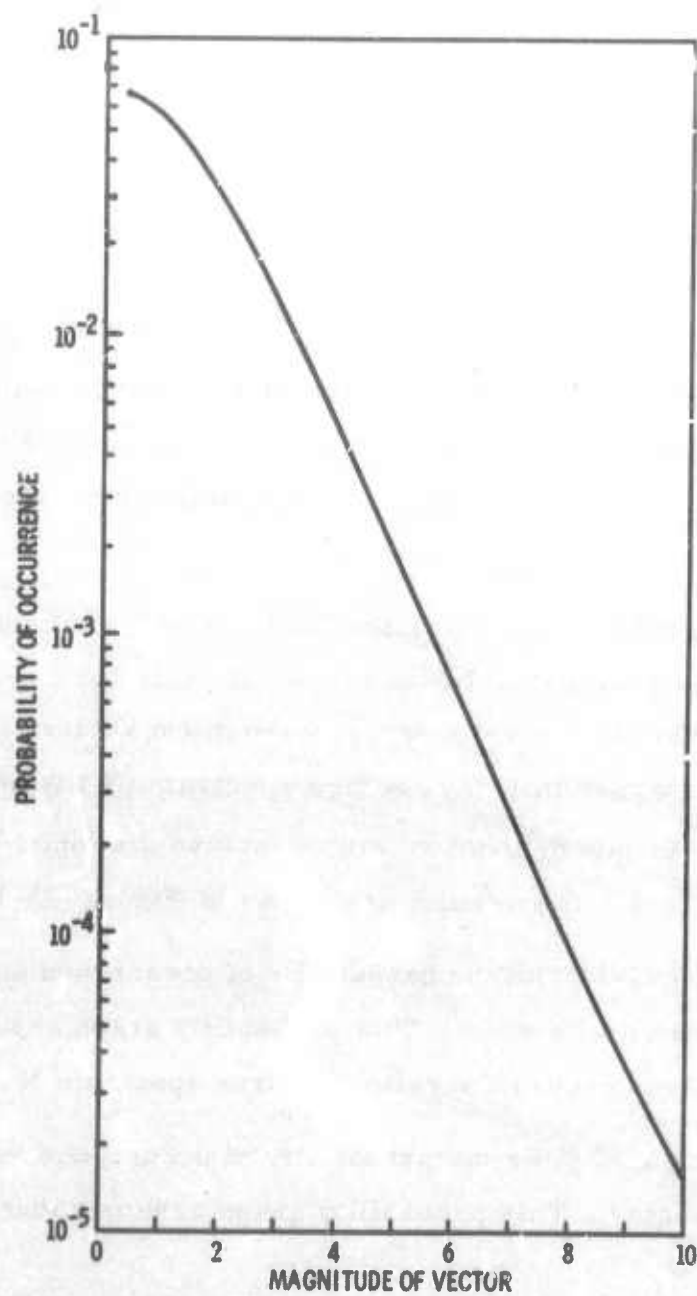
Figure II-1. False-Alarm Rate for 3-Dimensional Vector
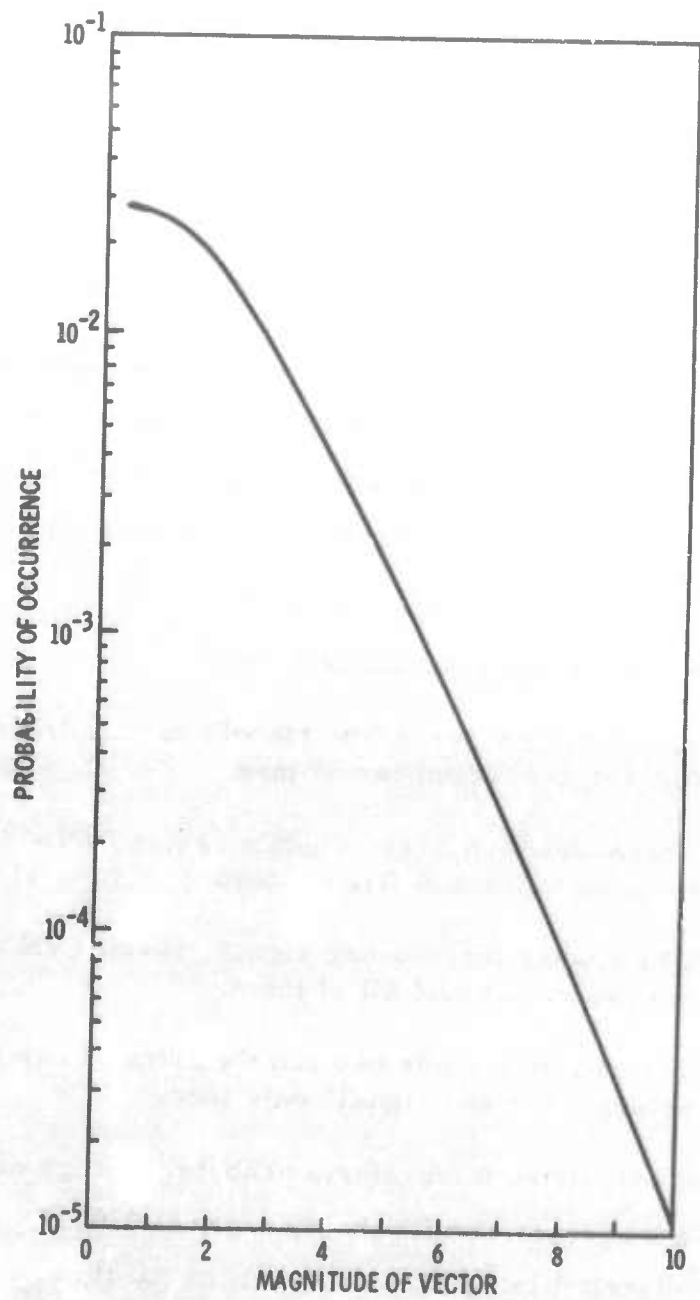
science services division

Figure II-2. False-Alarm Rate for 4-Dimensional Vector

A sample average power spectrum of one of these traces is shown in Figure II-3. An 80-point seismic wavelet having a power spectrum as shown in Figure II-3 and a waveform as shown in Figure II-4 is superimposed on the noise traces at signal-to-noise ratios of 0.7, 1.1, and 1.6 for a bandwidth of 0.62 to 1.72 cps after smoothing over two points. This bandwidth consists of three frequency points. The 12 traces of 4000-point length may be considered as a single 48,000-point, 80-min trace. Dividing this trace into 64-point blocks implies that there are 750 independent decisions as to whether both signal and noise are present or whether there is only noise.

The technique is then applied to the data, and the measured power spectra are smoothed over two points. A signal is considered detected in a segment of noise if the measured power spectrum exceeds the average over the bandwidth used and if the magnitude of the resulting vector exceeds 4.0.

The results are summarized below.

- There were seven 8-sec signals having S/N = 0.7; the program found two of them

- There were ten 8-sec signals having S/N = 1.1; the program found five of them

- There were three 8-sec signals having S/N = 1.6; the program found all of them

- The program made two false alarms, calling actual noise as "signal" only twice

The calculated false-alarm probability is given by 2/750 = 0.0027, which is in excellent agreement with the theoretical 0.0037. The program was able to detect the signals having S/N = 1.1 half of the time, doing better than the 0.27 expected for S/N = 1.0.
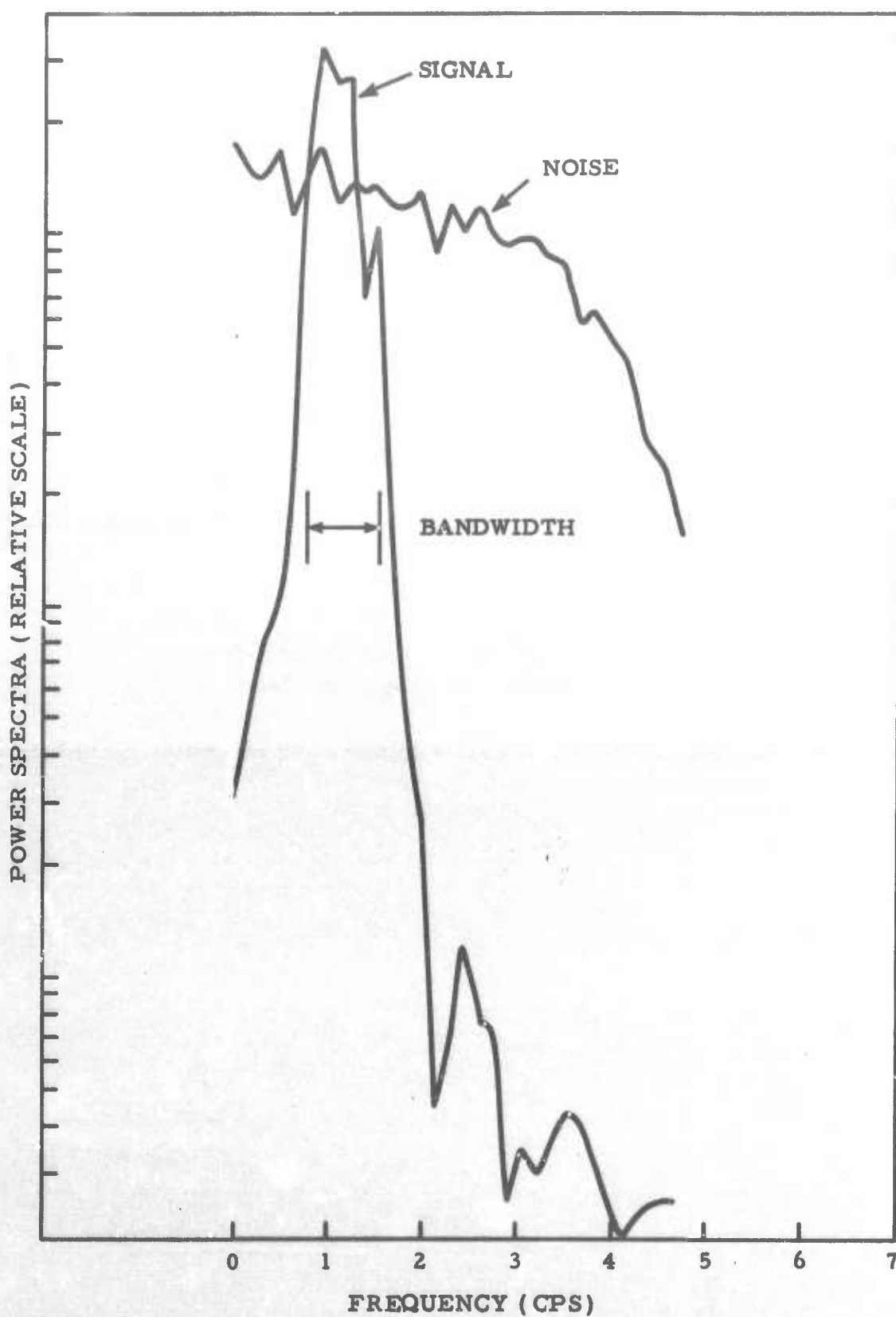
Figure II-3. Power Spectra of Gaussian Noise and
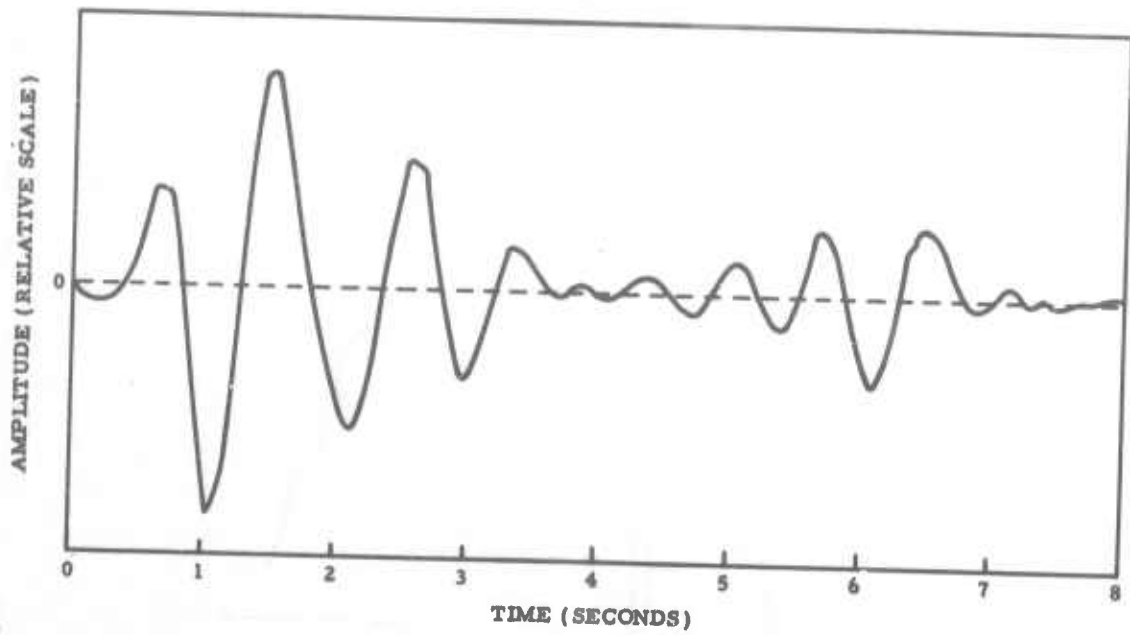Signal Superimposed on Gaussian Noise

Figure II-4.   Signal Used To Test Reliability of
Dynamic-Power-Spectra Method

science services division

SECTION III

APPLICATION OF METHODS TO LASA NOISE

The noise sample which was investigated for discrete arrivals was recorded at LASA on 25 March 1966 from 04:26: 12.8 to 04:34: 12.7. An antialiasing filter was applied to all noise recordings, and the resulting time traces then were decimated. This procedure yielded data traces 4800 points in length, with a sample rate of 0.1 sec.

To detect discrete arrivals propagating across the large array as plane waves, the outputs of the A, B, C, and D ring subarrays were used. B4 subarray was dead. These 12 subarrays were chosen because they were the closest within the large array (Figure III-1). Any signal would have had similar characteristics at all of these inner subarrays.

Reliability of the analysis of variance was initially investigated using 12 channels of generated random noise. The technique was applied to these traces with a time window of 6 sec. The maximum Fisher value obtained was 1.7, as indicated in the output time trace of Figure III-2. This value was used as the critical Fisher value; i.e., no signal was considered present in any segment of the noise unless the Fisher value of that segment was greater than 1.7. The actual critical value for a failure rate of 0.001, as determined by a table for the parameters used, was 1.67.

When this technique was applied to 12 channels of LASA noise data, it was found that the data should be deconvolved to obtain reasonable Fisher values. By deconvolving the time traces, the seismic noise is more nearly fitted to the model discussed in Section II; i.e., it more nearly satisfies the assumption that the observations in time are uncorrelated. This operation did not completely eliminate the correlations in time; therefore, the data did not realize the false-alarm rate of 0.001 for an F value of 1.67.

science services division
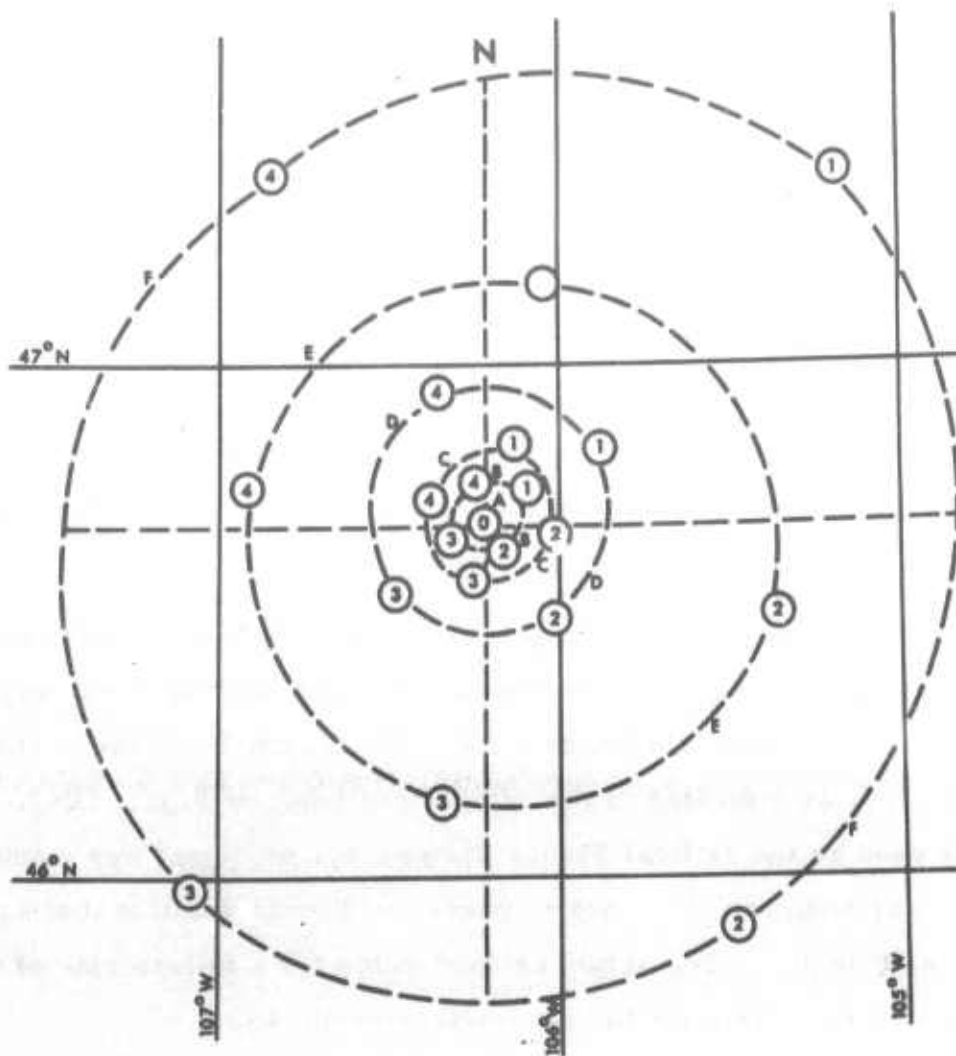
0 10 20 30 40 50 Km

November 1965

SUB–ARRAY "AO":
46° 41' 19" N
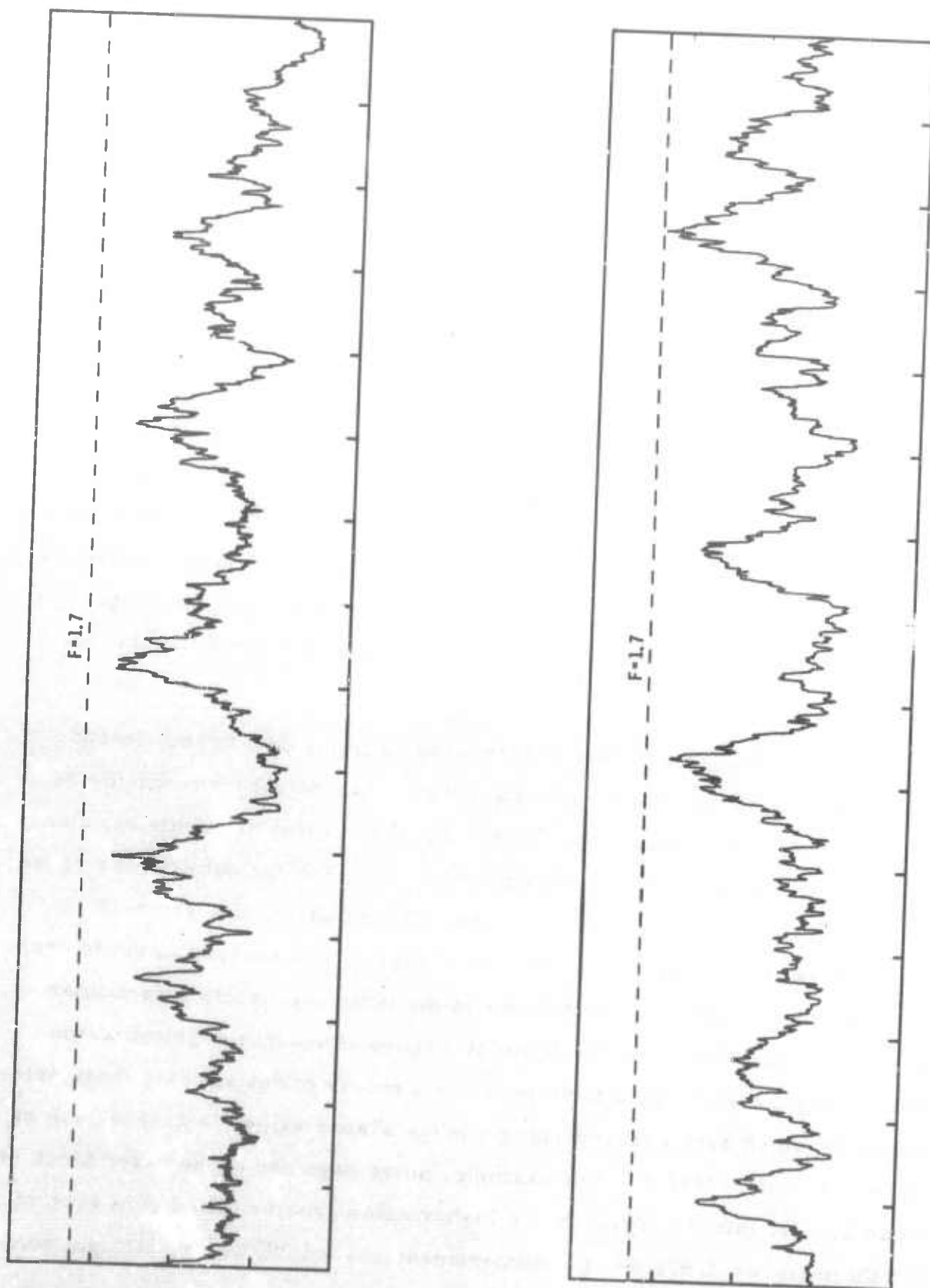106° 13' 20" W

LASA

Figure III-1.   LASA Subarrays

Figure III-2.   Fisher Time Trace for 12 Channels of Generated Random Noise

To use the analysis-of-variance technique on the large array, an output trace from each of the 12 inner subarrays was used. One such set of 12 traces was obtained by using a single seismometer output (trace 1 of ring 2, Figure III-3) from each of the subarrays. These traces were pre-whitened with a short (9-point) deconvolution filter designed on the output trace of subarray A0. This set of deconvolved noise was then beam-steered toward an area (NE China) which was known to be seismically active on 25 March and toward an area (S. Algeria) which was quiet. LASA travel-time anomalies were used in calculating the amount of time shift.

The analysis-of-variance method was applied to three sets of 12 traces: the data beam-steered to S. Algeria; the data beam-steered to NE China; and the nonshifted deconvolved data. A 6-sec time window was used. Figures III-4 through III-6 show the resulting Fisher time traces. The time scale on all traces is 20 sec/in., and the lower trace in each figure is a continuation of the upper trace. The dotted line represents the critical Fisher value of 1.7.

The Fisher trace corresponding to the data beam-steered toward the quiet zone (Figure III-4) and the Fisher output trace for the data which had not been time-aligned (Figure III-5) had three segments of noise each with values greater than the critical value. For the output trace of the data beam-steered toward the noisy area (Figure III-6), five segments had values above 1.7. Table III-1 lists the Fisher values corresponding to each of these noise segments. Each letter in the table represents a particular segment of the noise, and this letter is written above that segment on the Fisher output trace. This table provides a means of determining those noise segments which have correspondingly large Fisher values (> 1.7) in each of the Fisher output traces. For example, noise segment J, the 6-sec block of noise 255 sec into the trace, had a Fisher value greater than 1.7 in each of the three traces (i.e., traces beam-steered toward NE China, straight summed, and beam-steered toward S. Algeria).
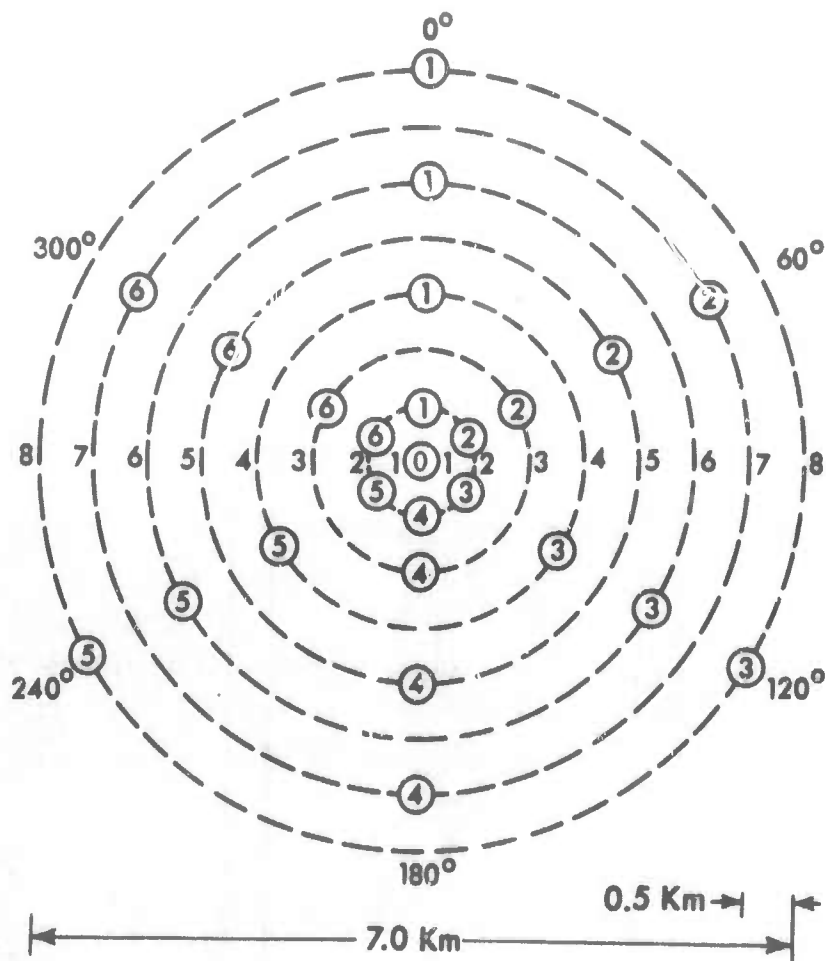
NOTE:
Seismometer No. 10 Is 500' Deep
Seismometers 21-65 Are 200' Deep

Figure III-3.   LASA Standard Subarray
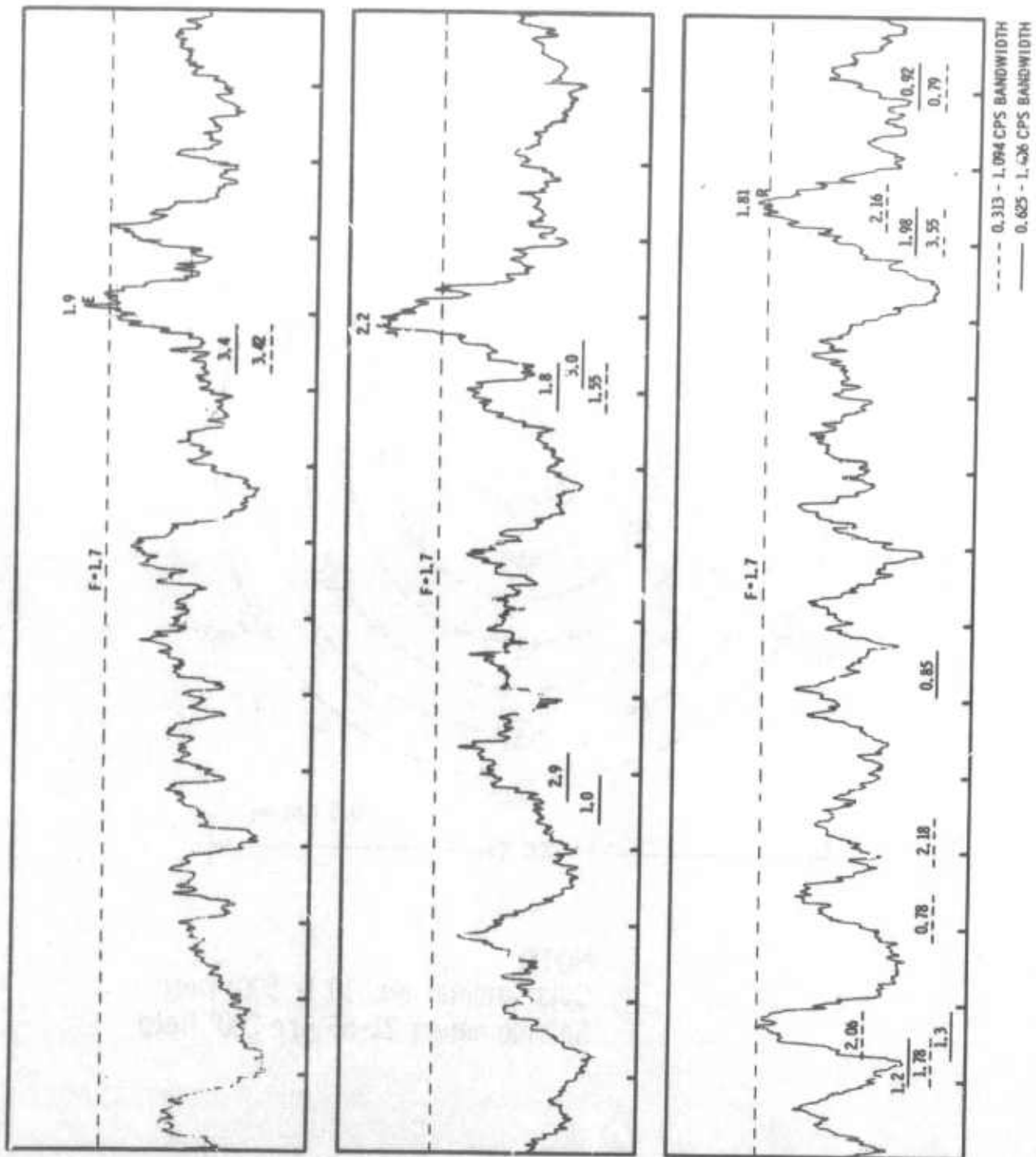
Figure III-4. Fisher Time Trace for Single Seismometer Outputs Beam-Steered toward S. Algeria

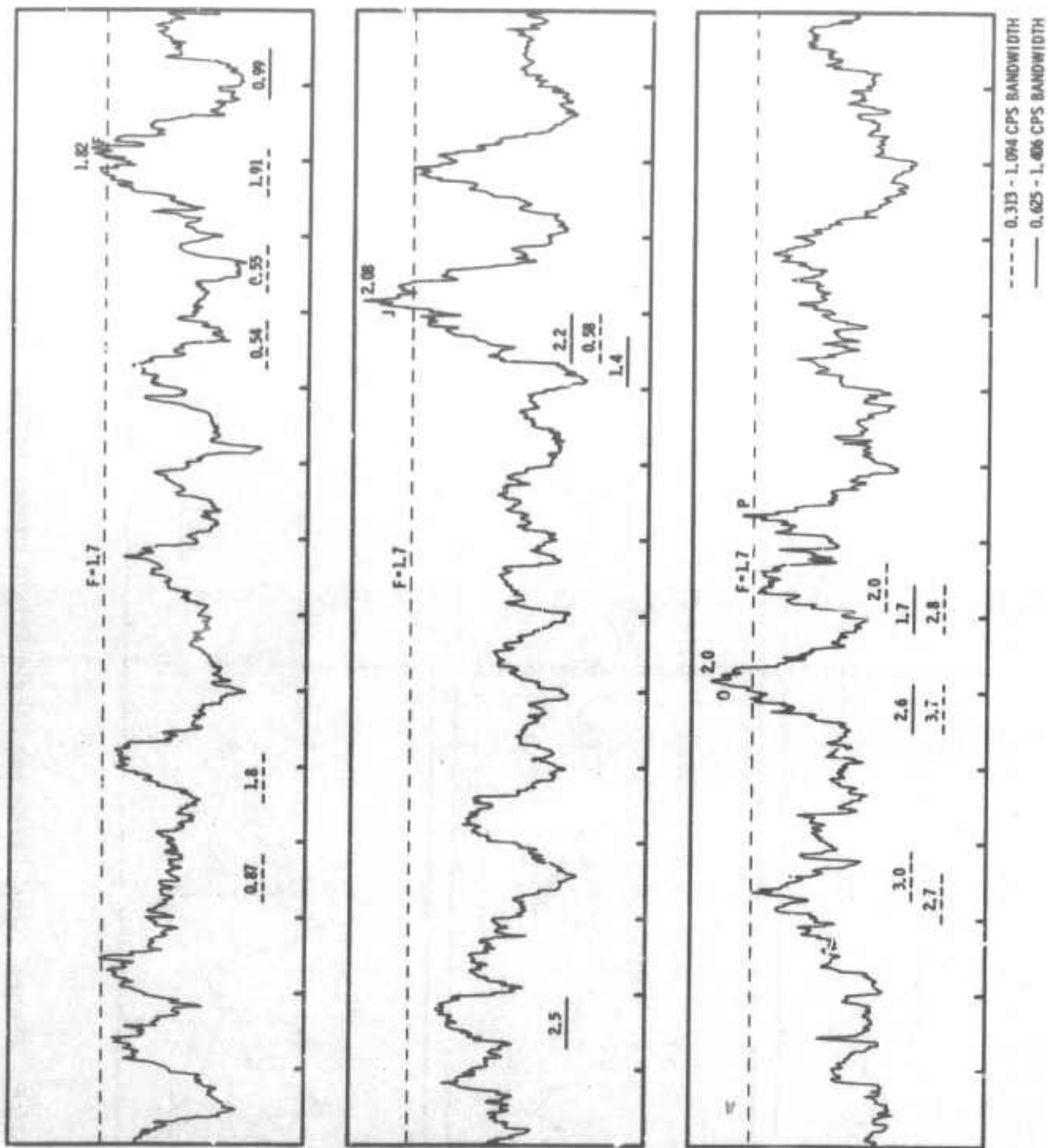science services division

Figure III-5. Fisher Time Trace for Single Seismometer Output (No Time Shift)

science services division
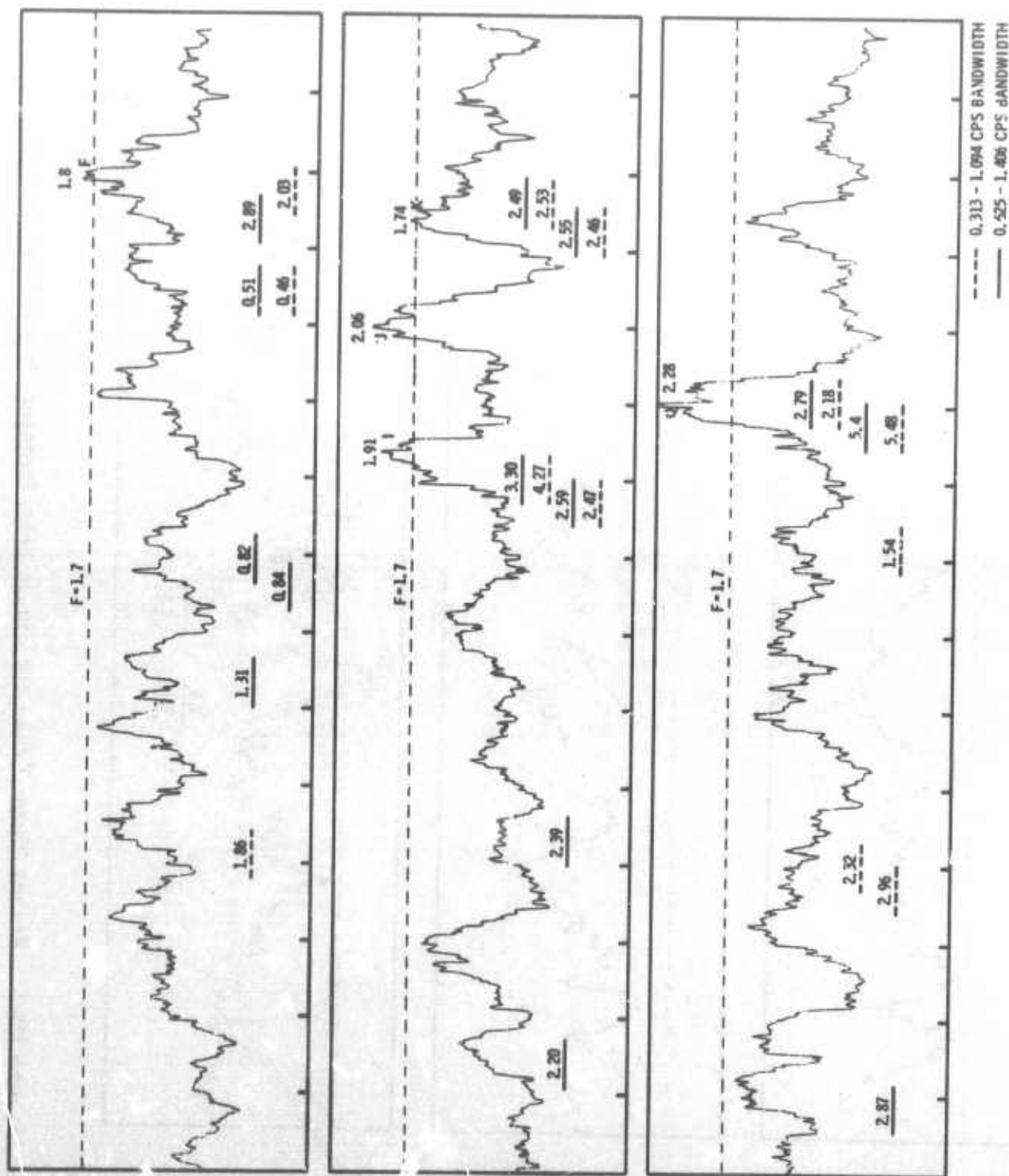
Figure III-6. Fisher Time Trace for Single Seismometer Outputs Beam-Steered toward NE China

science services division

Table III-1

RESULTS OF ANALYSIS-OF-VARIANCE
AND DYNAMIC-POWER-SPECTRA TECHNIQUES

64-Point Noise Segment	No Time Shift		S. Algeria			NE China		
	Trace 21	MCF	Trace 21	MCF	Straight Sum	Trace 21	MCF	Straight Sum
A (29)								$F=1.84$
B (82)			$F=2.1$			$M_2=0.82$		
C (84)							$F=1.85$	
D (91)			$F=1.8$					
E (111)			$F=1.9$			$M_1=0.46$ $M_2=0.51$		
F (130)	$F=1.82$ $M_1=1.9$				$M_1=0.77$	$F=1.8$ $M_1=2.03$		
G (155)		$F=2.06$						
H (178)					$F=1.77$ $M_1=3.5$			$F=1.79$ $M_1=1.86$ $M_2=2.01$
I (243)						$F=1.91$ $M_1=4.27$ $M_2=3.80$		$M_1=4.37$ $M_2=2.6$
J (259)	$F=2.08$ $M_2=2.2$		$F=2.2$	$F=1.84$		$F=2.06$		$M_2=0.6$
K (273)						$F=1.74$ $M_1=2.53$ $M_2=2.55$	$F=1.73$	$F=1.76$ $M_1=2.78$ $M_2=2.43$
L (292)							$F=1.73$	$F=2.11$ $M_2=2.34$
M (317)			$F=1.7$ $M_1=2.06$ $M_2=1.3$					$F=1.88$ $M_1=1.20$ $M_2=0.75$
N (358)							$F=1.76$	
O (363)	$F=2.0$ $M_1=3.7$ $M_2=2.6$		$M_2=0.85$					$F=1.74$
P (333)	$F=1.82$					$M_1=1.54$		$M_1=2.1$
Q (400)						$F=2.28$ $M_1=5.58$ $M_2=2.79$ $M_2=5.40$		$M_1=4.9$ $M_2=2.9$
R (425)			$F=1.81$ $M_1=2.16$ $M_1=3.55$ $M_2=1.98$		$M_1=3.0$			$M_1=1.8$

Fisher values > 1.7
M_1 = magnitude of vector for 0.313- to 1.094-cps bandwidth
M_2 = magnitude of vector for 0.625- to 1.406-cps bandwidth

These immediate results indicated that eight noise segments contained possible discrete arrivals since the Fisher values of those segments were greater than the critical value. To determine whether these noise segments contained discrete arrivals, two other sets of data from the 12 subarrays were investigated. A discrete arrival was considered present in a noise segment only if that segment had a Fisher value above 1.7 for all three sets beam-steered toward the same zone.

A multichannel filter system[6] was applied to the 25 noise traces within each subarray. The resulting 12 MCF time traces were prewhitened using a short deconvolution filter designed on the A0 MCF output. As in the previous case, the traces were beam-steered to two locations. Results of the analysis-of-variance technique are included in Figures III-7 through III-9 and in Table III-1.

In general, the Fisher traces obtained from the MCF outputs contained fewer noise segments with Fisher values above the critical value than did the Fisher traces obtained using single-seismometer outputs. Also, the Fisher values for a particular MCF set were smaller than those of the corresponding individual-seismometer Fisher trace. Since the MCF outputs were velocity-limited, the large number of high Fisher values from the single-seismometer output may have been the result of surface-mode energy. The noise data had not been low-cut-filtered to eliminate the microseism peak energy.

The MCF Fisher output trace for the nonshifted data (Figure III-7) contained only one segment of noise with a Fisher value of sufficient magnitude to indicate an arrival. This segment, however, did not correspond to any of the noise segments in the nonshifted individual seismometer output trace (Figure III-5) which contained possible arrivals. For the data beam-steered toward S. Algeria, there was one agreement between peaks in the Fisher values of the MCF output trace (Figure III-8) and the single-seismometer trace;

this occurred for noise segment J, a segment 260 sec from the beginning of the data. Also, there was only one peak corresponding in the Fisher traces for the MCF traces and the individual seismometer traces beam-steered toward NE China. Thus, two noise segments contained possible discrete arrivals.

The third set investigated by this method was a straight-sum output of the 25 traces within each subarray. These 12 traces were pre-whitened and beam-steered as in the other two cases. The analysis-of-variance technique was applied with a 6-sec time window. Figures III-10 and III-11 show the Fisher output traces.

There were seven segments of noise with Fisher values above 1.7 beam-steered to NE China. For the straight sums beam-steered toward S. Algeria (the quiet zone), only one segment of noise had a value (1.77) greater than the critical value. There was no agreement between this segment (of the S. Algerian data) and noise segment J which had a large Fisher value in the corresponding individual-seismometer output and the MCF output. However, when the Fisher traces were investigated for discrete arrivals by comparing the three traces which had been beam-steered toward NE China, one segment was found to consistently have large F values. For these data (Figures III-6, III-9, and III-11), one segment 275 sec into the record had a peak F value when the values were calculated using the individual-seismometer, straight-sum, and MCF outputs. Thus, the analysis-of-variance technique which was applied to a portion of the large array detected a possible discrete mantle P-wave arrival in the noise when the data were beam-steered toward NE China.

The dynamic-power-spectra technique was also used to try to detect discrete arrivals traveling across the large array as plane waves. This method was applied to five single traces obtained by summing the 12 traces within each of five sets used in the analysis-of-variance study.
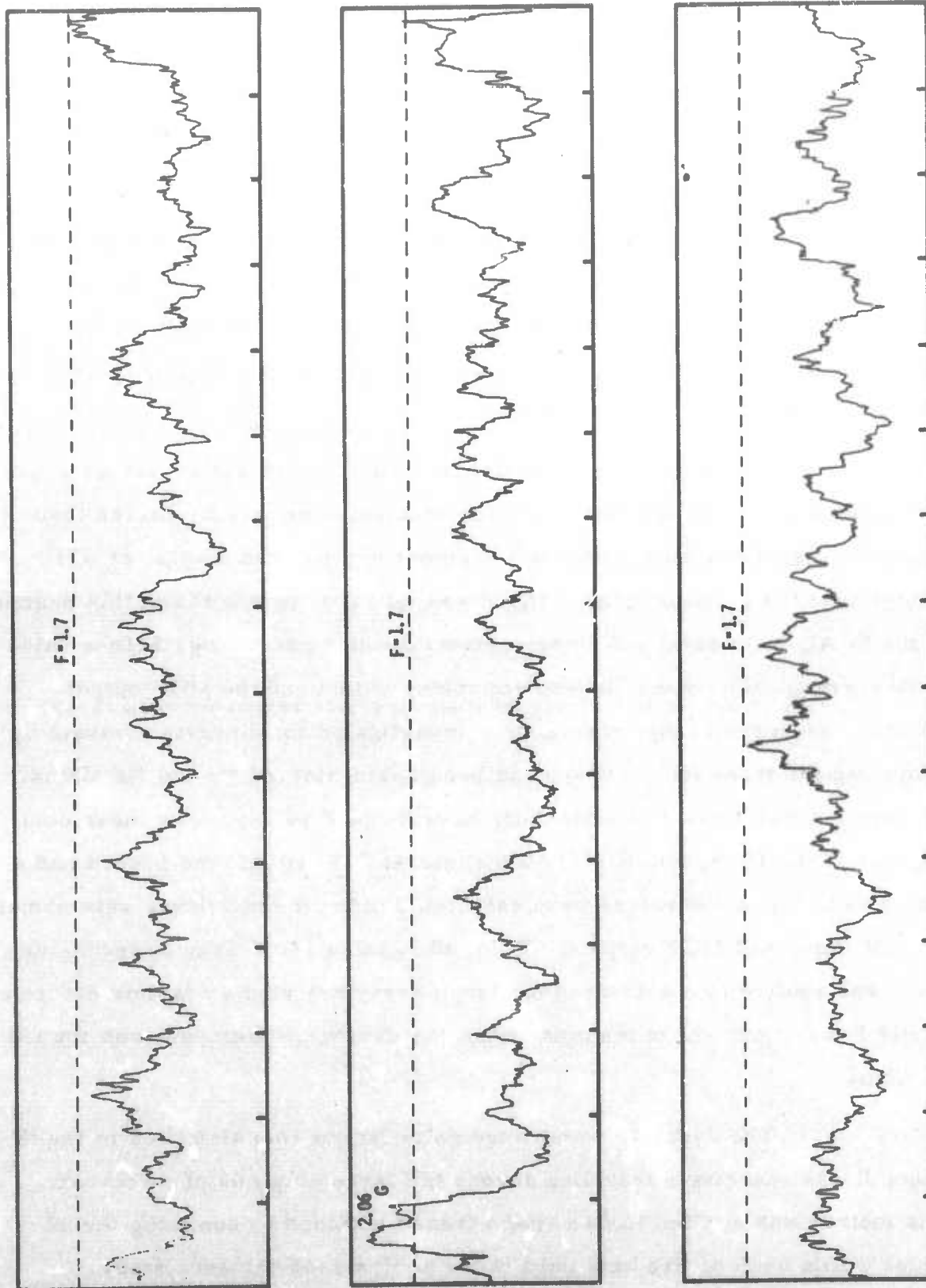
Figure III-7. Fisher Time Trace of MCF Outputs (No Time Shift)

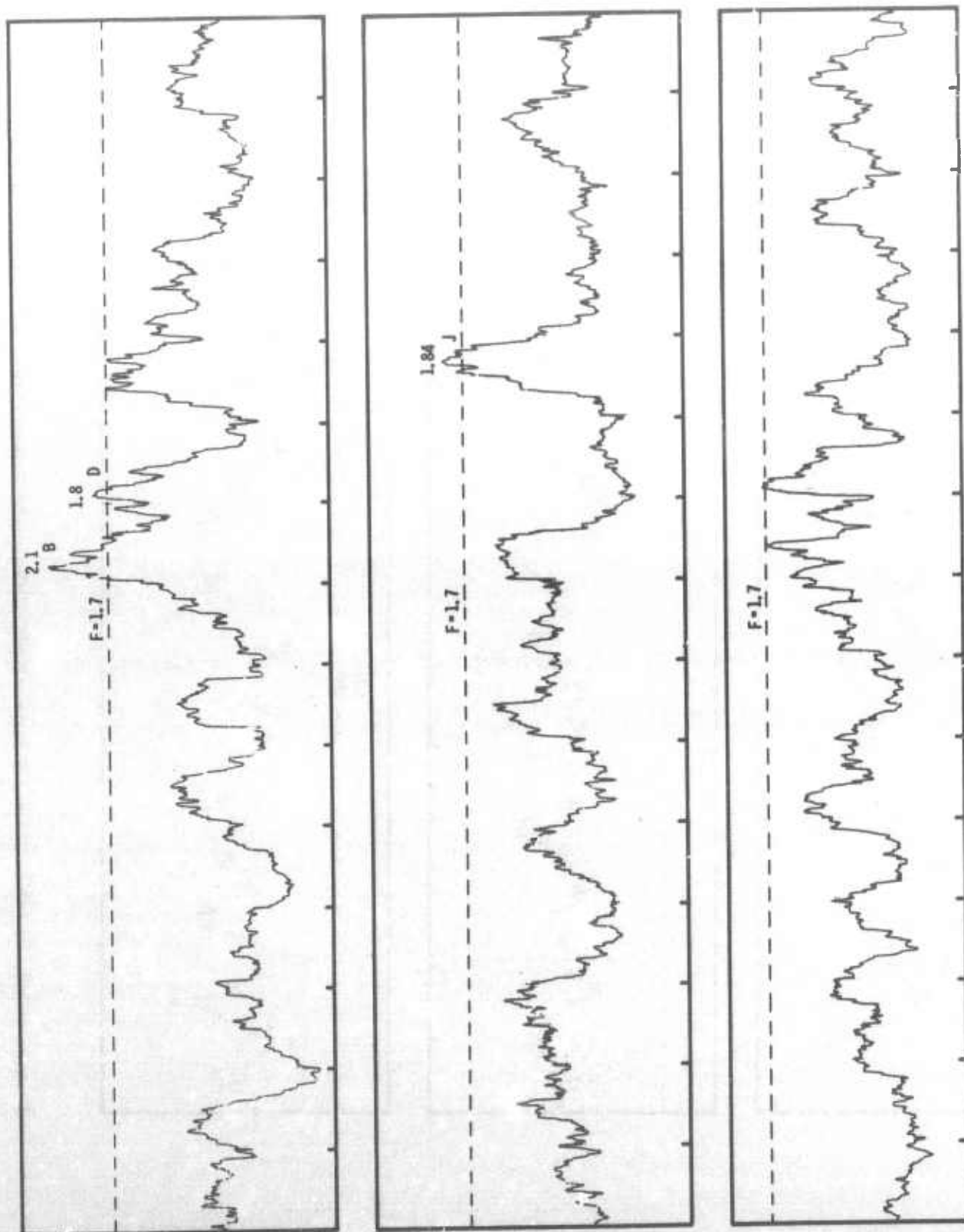Figure III-8. Fisher Time Trace of MCF Outputs Beam-Steered toward S. Algeria.
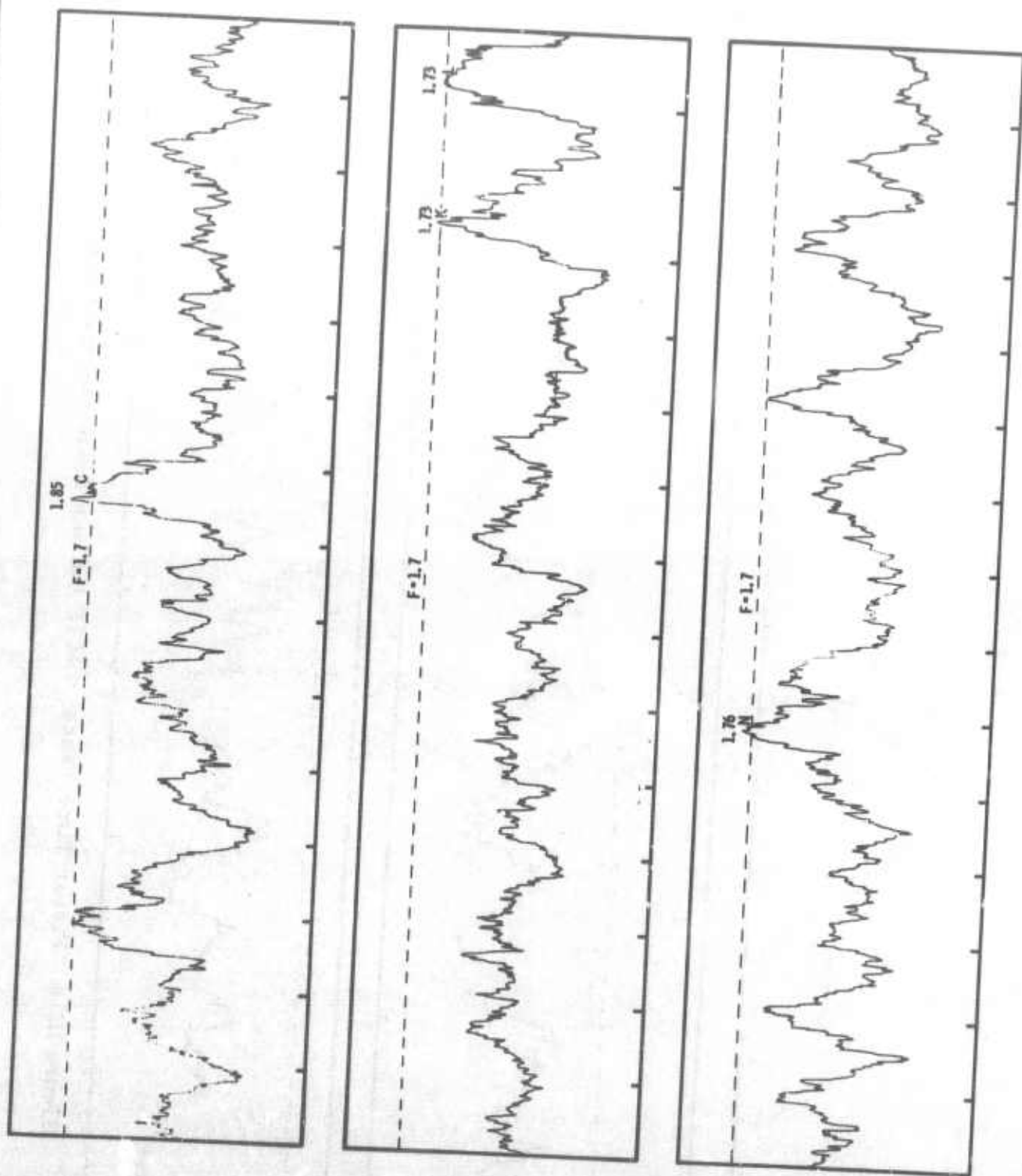
Figure III-9. Fisher Time Trace of MCF Outputs Beam-Steered toward NE China

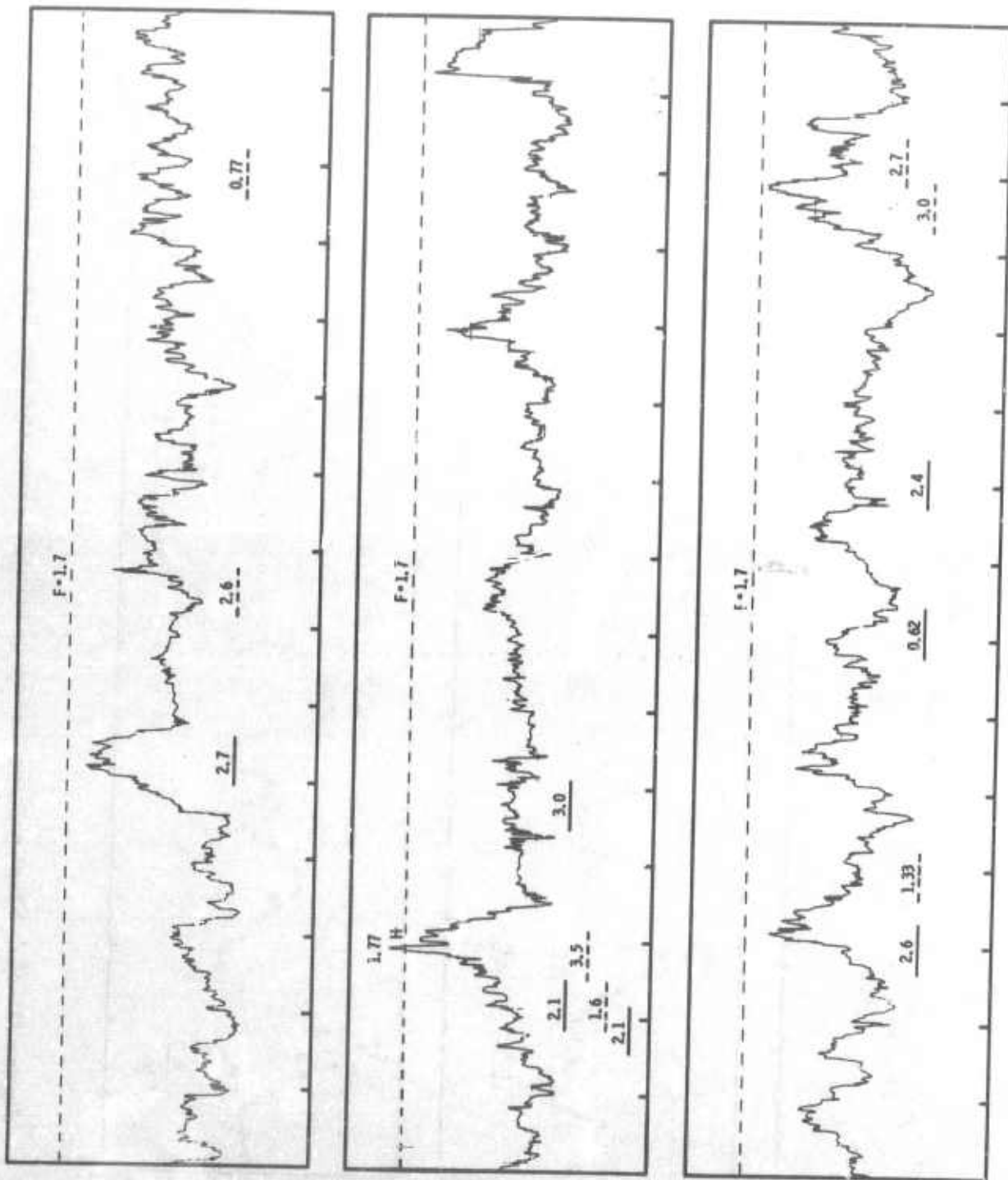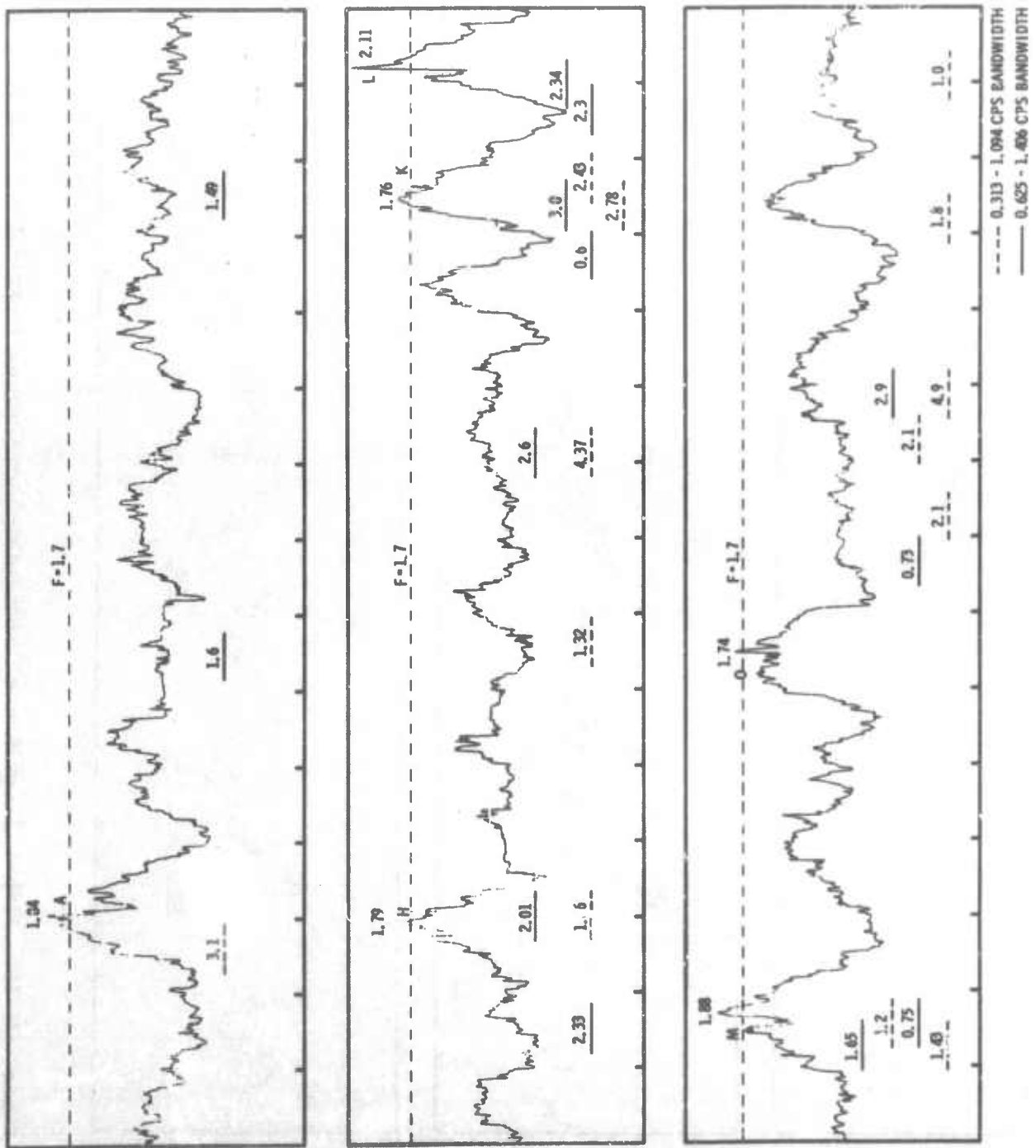Figure III-10. Fisher Time Trace of Straight-Sum Outputs Beam-Steered to S. Algeria

--- 0.313 - 1.094 CPS BANDWIDTH
— 0.625 - 1.406 CPS BANDWIDTH

science services division

Figure III-11. Fisher Time Trace of Straight-Sum Outputs Beam-Steered to NE China

The MCF outputs were not summed. Specifically, three traces for the individual-seismometer outputs (NE China, S. Algeria, no shift) and two traces for the straight-sum outputs (NE China, S. Algeria) were used. The measured power spectra were smoothed over two frequency points and investigated in the frequency bandwidths of 0.313 to 1.094 cps and 0.625 to 1.406 cps. These frequency ranges correspond to a 3-dimensional vector having a false-alarm probability curve as shown in Figure II-1. Results of this method have been superimposed on the Fisher output trace of Figures III-4 through III-6 and Figures III-10 and III-11. The bars below the traces indicate the 64-point noise segments with measured power spectrum exceeding the average power spectrum over the bandwidths used. The magnitude of the vector is shown above each bar.

According to Figure II-1, the probability of occurrence of a 3-dimensional vector with a magnitude greater than 4.0 is less than 0.005. Initial results of this method when applied to LASA noise over the large array indicate that a reliable analysis can be made if vectors with magnitudes of 2.5 are considered. The corresponding probability of occurrence for 3-dimensional vectors with magnitudes above this is less than 0.019. Therefore, analysis of the dynamic-power-spectra method is based mainly on vector magnitudes greater than 2.5

The dynamic-power results for the individual-seismometer outputs beam-steered to S. Algeria (Figure III-4) contained four segments of noise with vector magnitudes exceeding 2.5 for the two bandwidths considered. For the bandwidth of 0.313 to 1.094 cps, one segment of noise with magnitude 3.55 corresponded to a peak in the Fisher output trace. The other three segments, however, did not correspond to any peaks with Fisher values above 1.7. In particular, the measured spectra of noise segment J, at 259 sec with a maximum Fisher value of 2.2, did not exceed the average spectra for the frequencies within the two bandwidths.

For the individual-seismometer outputs which were not beam-steered, this method resulted in six magnitudes above 2.5. One segment with a Fisher value of 2.0 had a corresponding vector of magnitudes 3.7 and 2.6 for the bandwidths of 0.313 to 1.094 cps and 0.625 to 1.406 cps, respectively. There was no agreement between the other peaks and vectors. These results are illustrated in Table III-1. The third trace (single-seismometer outputs beam-steered toward NE China) had 11 magnitudes greater than 2.5; seven of these vectors corresponded to Fisher values above the critical value. The segment of noise having the largest Fisher value also had the largest vector magnitudes in both bandwidths. Noise segment K had four corresponding vectors with magnitudes above 2.4. In all cases, most vectors of large magnitudes (> 2.0) corresponded to peaks in the Fisher time traces, although the values of these peaks were below 1.7.

The dynamic-power-spectra technique was applied also to the sum of the straight sums of the individual seismometers beam-steered to NE China and to the sum of the straight sums beam-steered to S. Algeria. For the NE China data, three segments of noise for the bandwidth of 0.313 t 1.094 cps and three segments for the bandwidth of 0.625 to 1.406 cps had magnitudes above 2.5. One of these segments, which had a vector magnitude above 2.5 for both bandwidths, corresponded to noise segment K having a Fisher value of 1.76. For the data beam-steered toward S. Algeria, there were three vectors of magnitudes above 2.5 in the bandwidth of 0.313 to 1.094 cps and two in the bandwidth of 0.625 to 1.406 cps. Of these, only one (with a magnitude of 3.5) corresponded to a Fisher value above the maximum value of the random noise data.

Comparing the results of the dynamic-power-spectra method for the three sets of output traces, only one consistent agreement between the location of the arrivals was noted. In other words, for one segment of noise,

the power spectra exceeded the average power at the three frequencies within the two bandwidths and the vector magnitudes were greater than 2.5 for both the individual-seismometer outputs and the straight-sum outputs. This particular segment occurred in the NE China data.

It was expected that, if a discrete arrival were detected within the same segment of noise by both methods, an arrival would be present in the noise. This occurred only for noise segment K for the data beam-steered to NE China. Fisher values were above 1.7 for this segment in the MCF, straight-sum, and single-seismometer outputs, and the magnitudes of the vectors corresponding to this segment were greater than 2.5. Thus, the large-array study indicated a discrete arrival from NE China, behaving as would be expected of a small signal from teleseismic distances.

In investigating the large-array outputs, the wave velocity was a critical factor since the maximum separation between the subarrays was 54 km. Thus, only a very limited region of wavenumber space could be investigated for discrete P-wave arrivals by any one set of time shifts. In order to have general simultaneous coverage of the high-velocity field, the two detection techniques were applied to output traces of individual subarrays. The 13 seismometers on the four inner rings (Figure III-3) were used to make the methods less velocity-sensitive. Only the outputs of the four subarrays A0, B1, B2, and B3 were studied. To remove the effects of microseisms at lower frequencies, the noise recordings were bandpass-filtered (0.8- to 5.0-cps bandpass). These filtered outputs were then prewhitened using a 9-point deconvolution filter designed on trace 21 of each subarray.

To estimate the power of both methods for the detection of discrete arrivals within a subarray, a 5-sec signal which had been bandpass-filtered and deconvolved was superimposed on the 13 filtered inner traces of subarray B1. The same signal waveform was added to each trace (filtered signal shown in Figure III-12). The signal was buried within the 8-min noise sample at six different positions corresponding to six velocities of propagation.
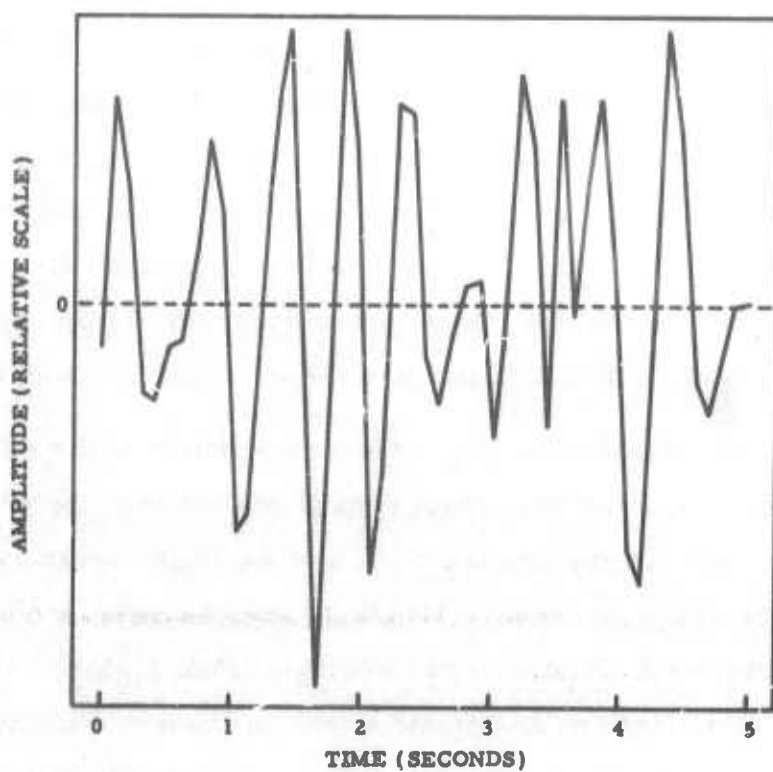
Figure III-12. Signal Used to Test Reliability of
Analysis-of-Variance Techniques

The signal was superimposed on the noise with signal-to-noise ratios of approximately 1 and 1/2   To do this, the signal was scaled by a factor determined by dividing the maximum value of the noise segment by the maximum value of the signal.   Figure III-13 shows a segment of the time traces containing the signal with an S/N = 1/2 and a velocity of 14 km/sec.

The Fisher analysis-of-variance method, using a time window of 3 sec, was applied to the 13 traces containing the embedded signals.   The output trace is shown in Figure III-14.   This method was able to detect all signals with S/N = 1/2 or larger and a velocity greater than 10 km/sec.   The dotted line across the trace in Figure III-14 corresponds to the maximum F value obtained when the analysis of variance was applied to the 13 traces before the signals were superimposed.   Fisher values for the segments containing a signal ranged from 4.0 to 12.17.

The dynamic-power-spectra technique also was applied to one of the traces containing the embedded signal.   Three bandwidths — 0.625 to 1.406 cps, 1.25 to 2.031 cps, and 0.938 to 1.719 cps — were used; each contained three frequency points.   The outputs of this method are superimposed on the Fisher output time trace in Figure III-14.   The number of successful detections varied among the three bandwidths, but the 1.25- to 2.031-cps range detected more of the signals.   There were only two false alarms: one in the 0.625- to 1.406-cps bandwidth with a magnitude of 2.7 and the other in the 1.25- to 2.031-cps bandwidth with a magnitude of 1.13.   (The latter false alarm is not shown in the figure since it occurred on the last part of the trace away from a signal.)   These two magnitudes corresponded to false-alarm probabilities of 0.018 and 0.044.   It should be noted that the results of the dynamic-power-spectra technique were not affected by the wave velocity of the signals in this experimental case since only one of the individual traces was used.   Therefore, the results of this method on the experimental signal were studied for the number of signals detected and the signal-to-noise ratios.
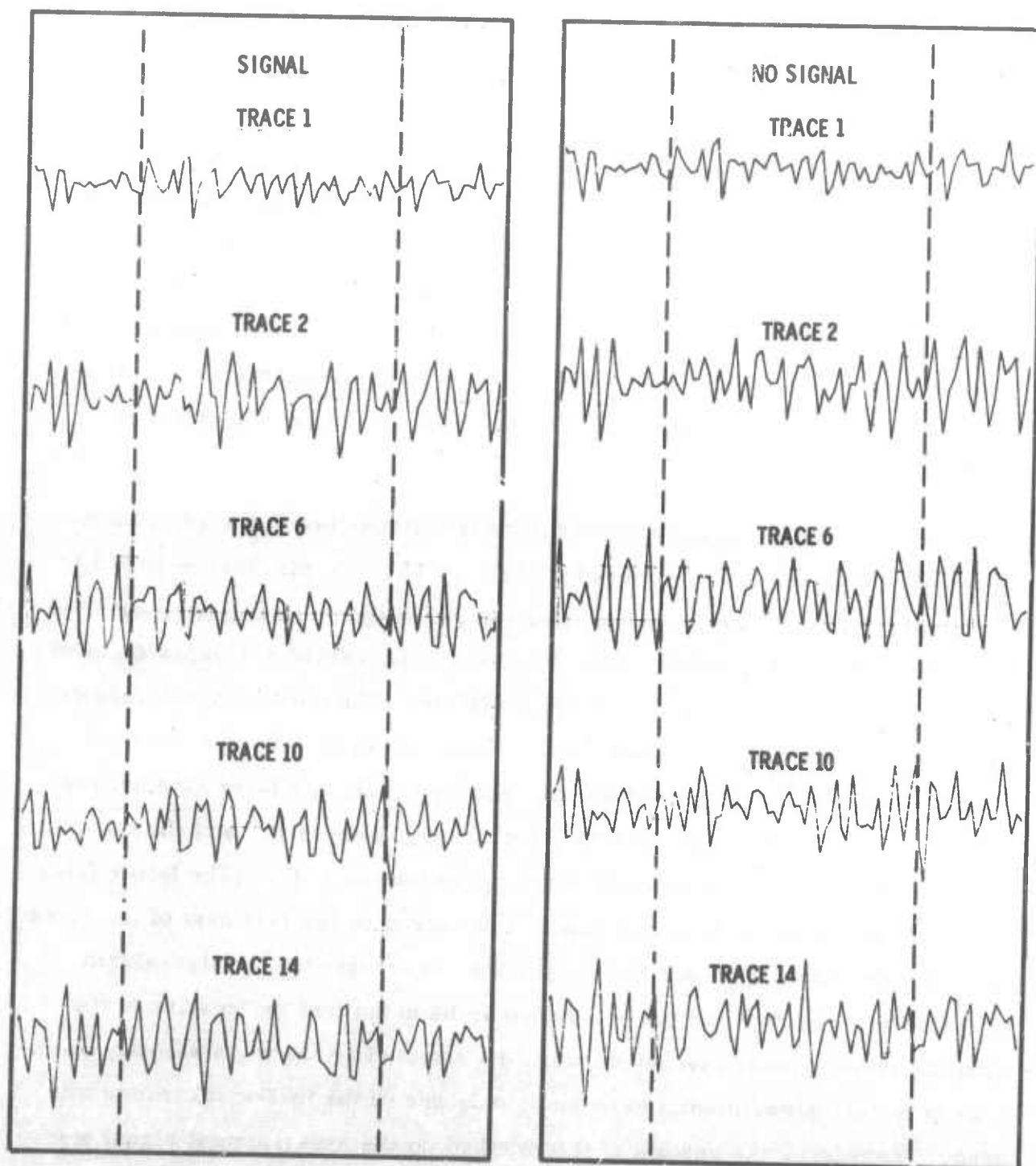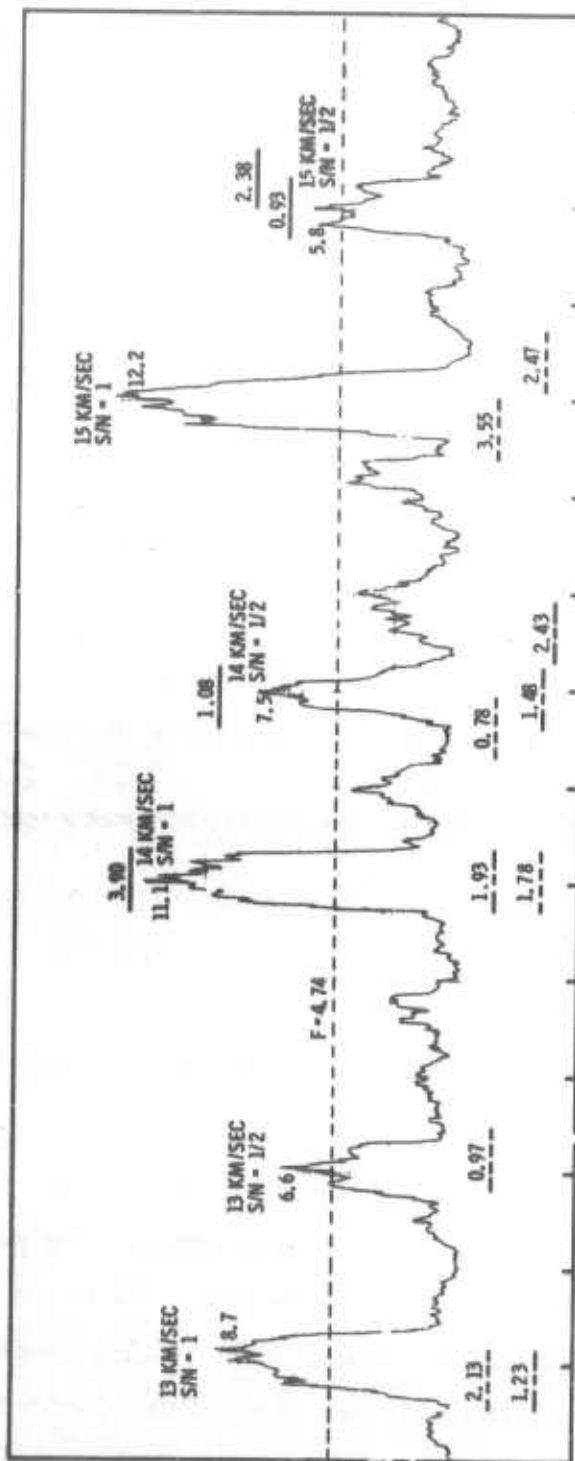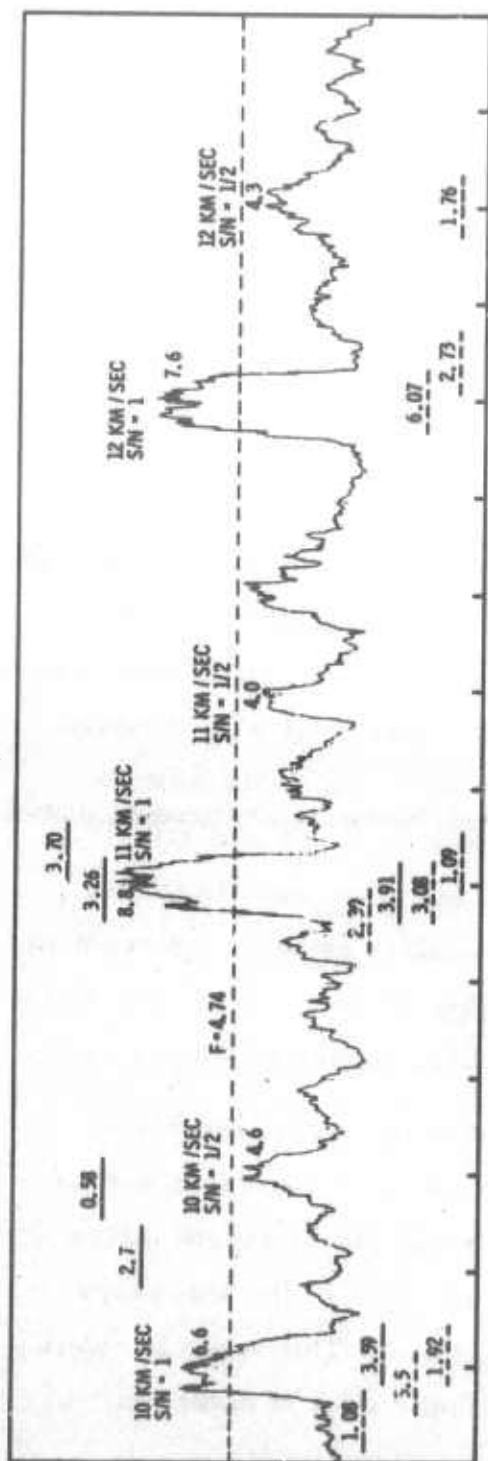
Figure III-13. Signal Superimposed on Noise of Subarray B1

Figure III-14. Fisher Time Trace of Noise Containing Embedded Signals

science services division

This test indicated that both the analysis-of-variance method and the dynamic-power-spectra technique should detect discrete P-wave arrivals which have a $\Delta > 30°$ and a signal-to-noise ratio of 1/2 or larger and are highly coherent.

The analysis-of-variance technique was applied to the 13 filtered inner traces of the four subarrays for the same noise used in the large-array analysis. A 3-sec time window was used. Resulting Fisher time traces are shown in Figures III-15 through III-18. For subarray A0, eight segments of noise had Fisher values above 3.0. The maximum value was 3.83, which was below the minimum value (4.0) obtained in the test case for a signal traveling at 11 km/sec with S/N = 1/2. In subarray B1 shown in Figure III-16, four segments of noise had Fisher values between 4.0 and 4.74. These values, compared to the results of the embedded signal output trace, indicated four possible discrete arrivals. There were also four Fisher values larger than 4.0 in the output trace of subarray B2 (Figure III-17), although the largest value was only 4.15. Two possible discrete arrivals were detected in subarray B3, corresponding to Fisher values of 4.4 and 9.09 (Figure III-18). The largest value should be highly significant and should, in fact, be visible in the time traces of B3. Figure III-19 contains the segment of the 13 filtered traces corresponding to this large Fisher value. The signal was clearly present. A small spike appears to have caused this large value.

If a discrete arrival were present in the noise, the Fisher time traces should have a large value for this segment in all four subarray outputs. Therefore, to determine if the peaks in the Fisher output traces corresponded to the same segments of noise within each of the subarrays, a straight sum of the four Fisher traces was calculated. This trace is shown in Figure III-20. The sum indicated only two possibilities of detection.
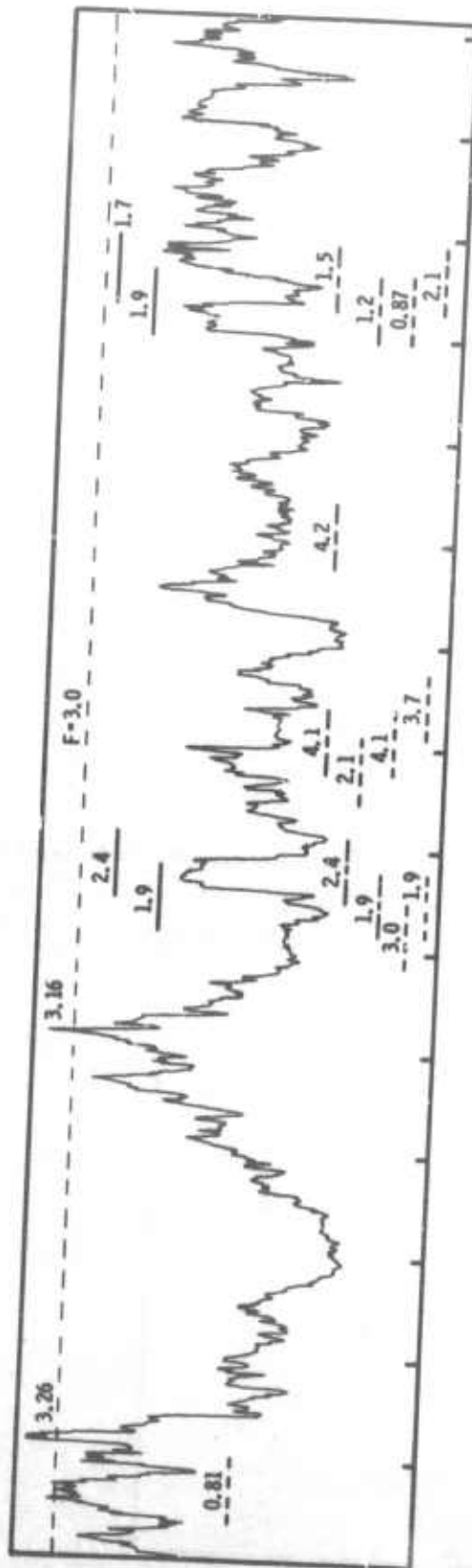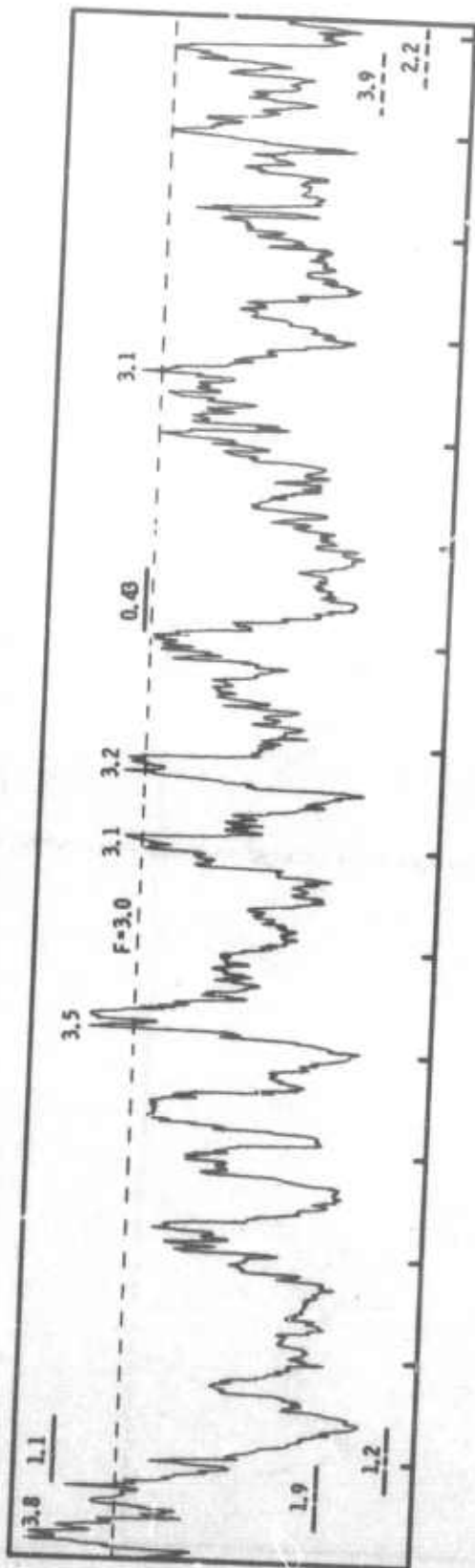
Figure III-15. Fisher Time Traces for Filtered Traces of Subarray A0

——— 0.625 - 1.406 CPS BANDWIDTH
——— 1.25 CPS - 2.01 CPS BANDWIDTH
——— 0.938 - 1.719 CPS BANDWIDTH

Figure III-16. Fisher Time Traces for Filtered Traces of Subarray B1

——— 0.625 - 1.406 CPS BANDWIDTH
- - - 1.25 - 2.031 CPS BANDWIDTH
— - — 0.938 - 1.719 CPS BANDWIDTH

Figure III-17. Fisher Time Traces for Filtered Traces of Subarray B2

——— 0.625 - 1.406 CPS BANDWIDTH
- - - - 1.25 - 2.031 CPS BANDWIDTH
— - — 0.938 - 1.719 CPS BANDWIDTH

science services division

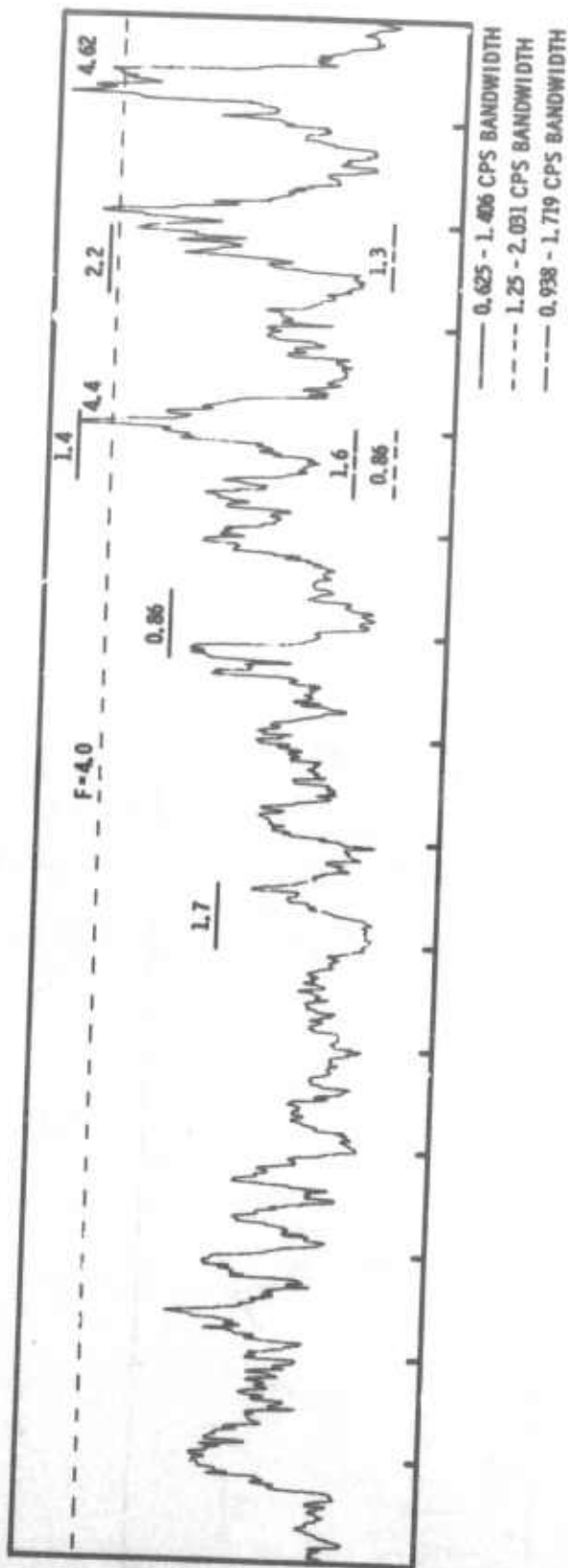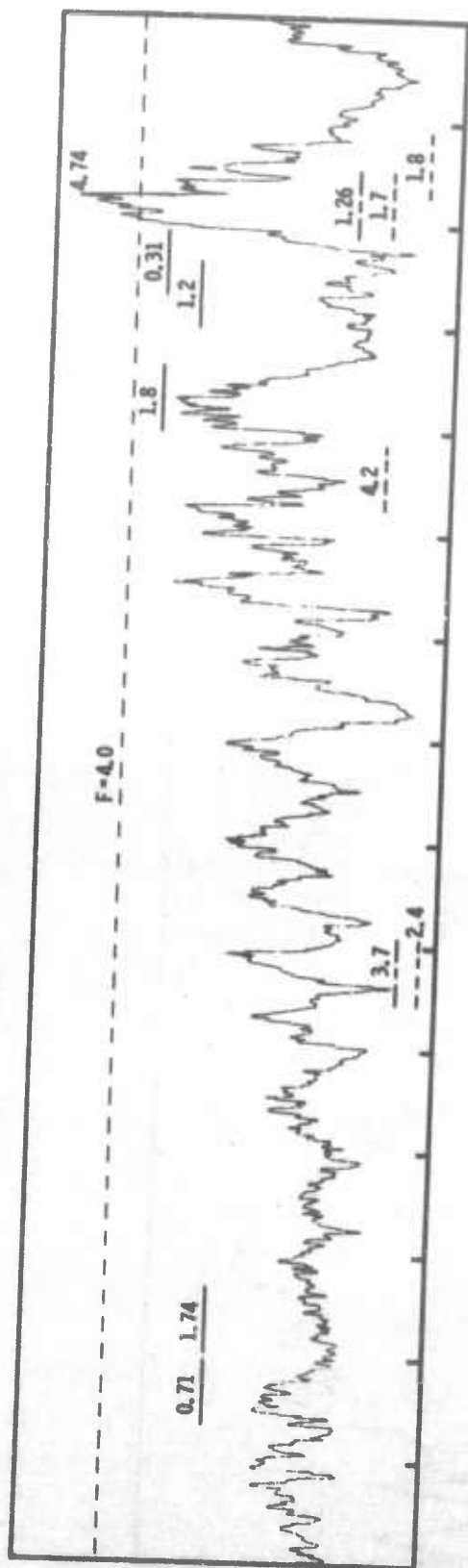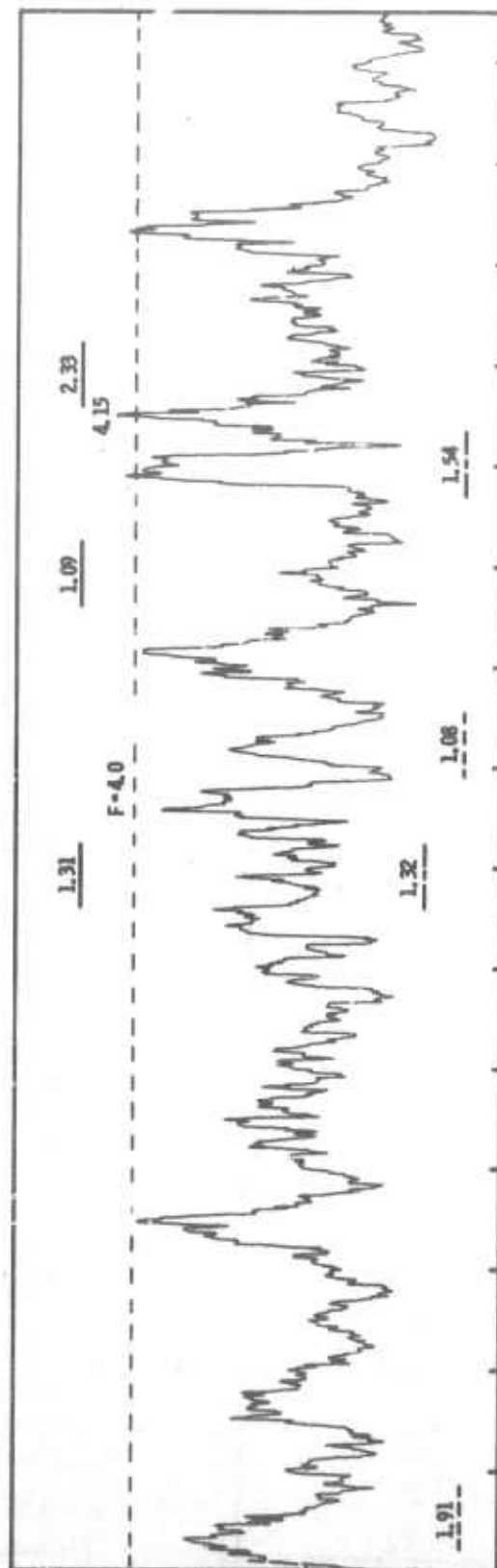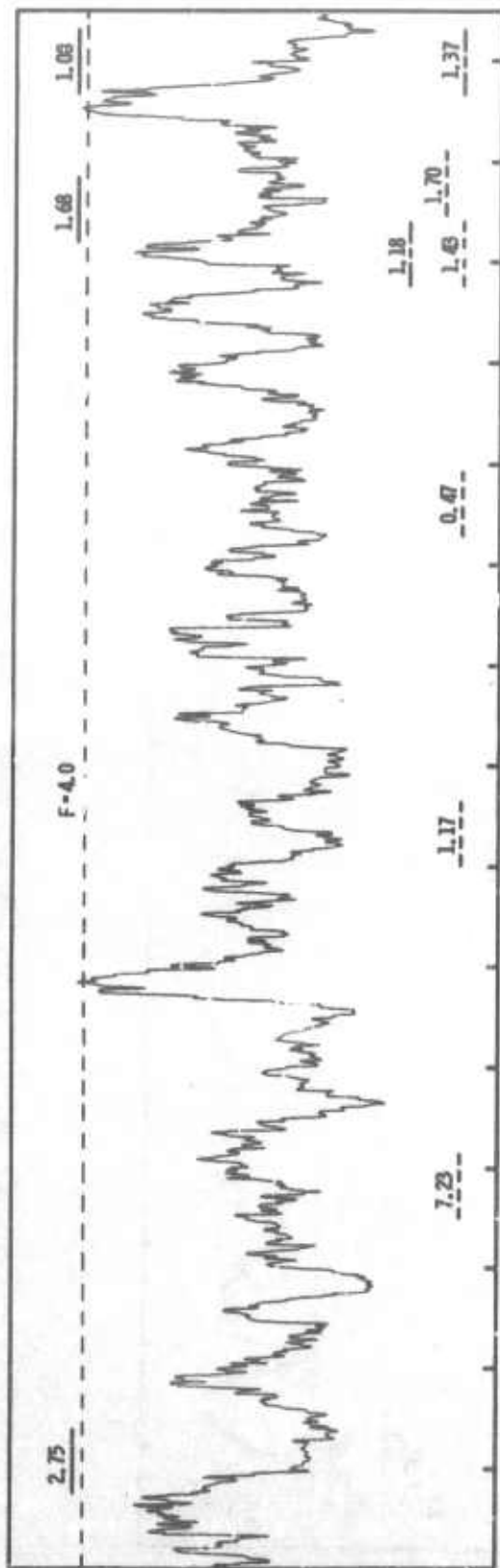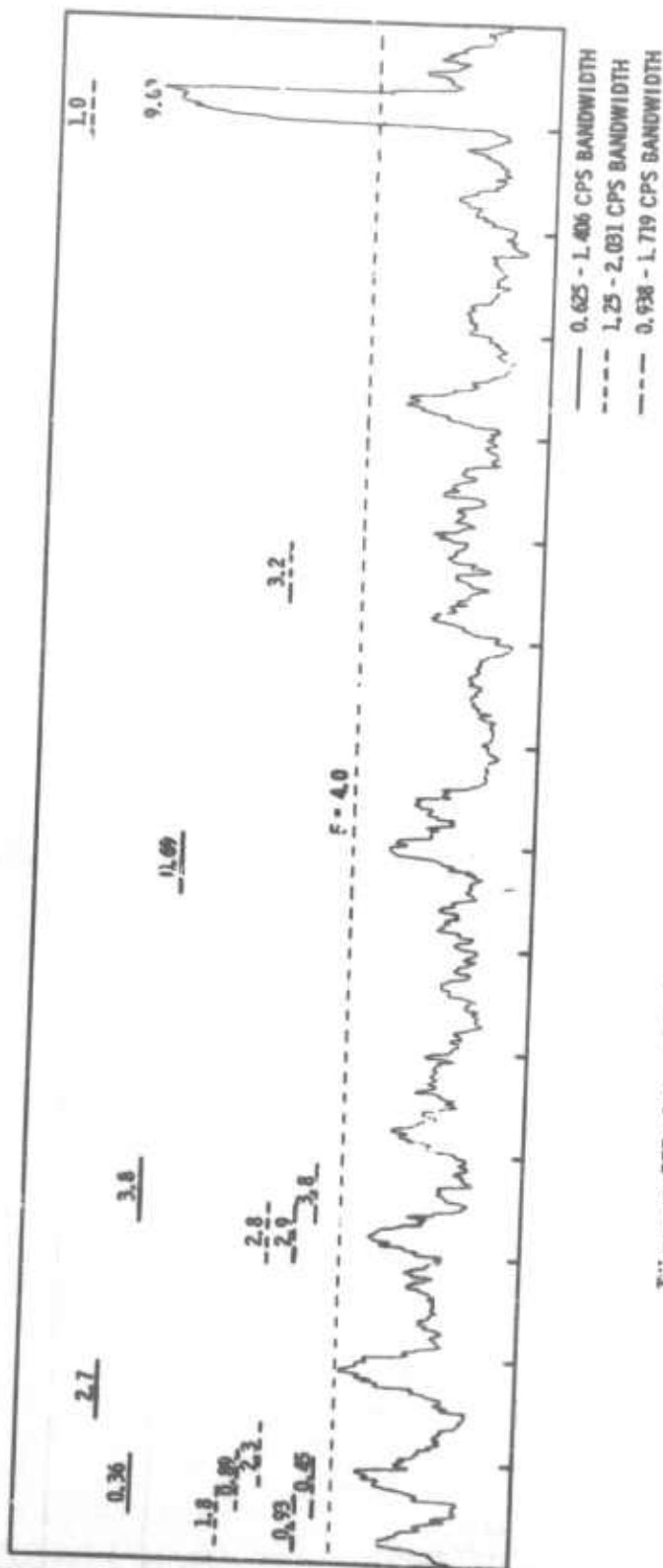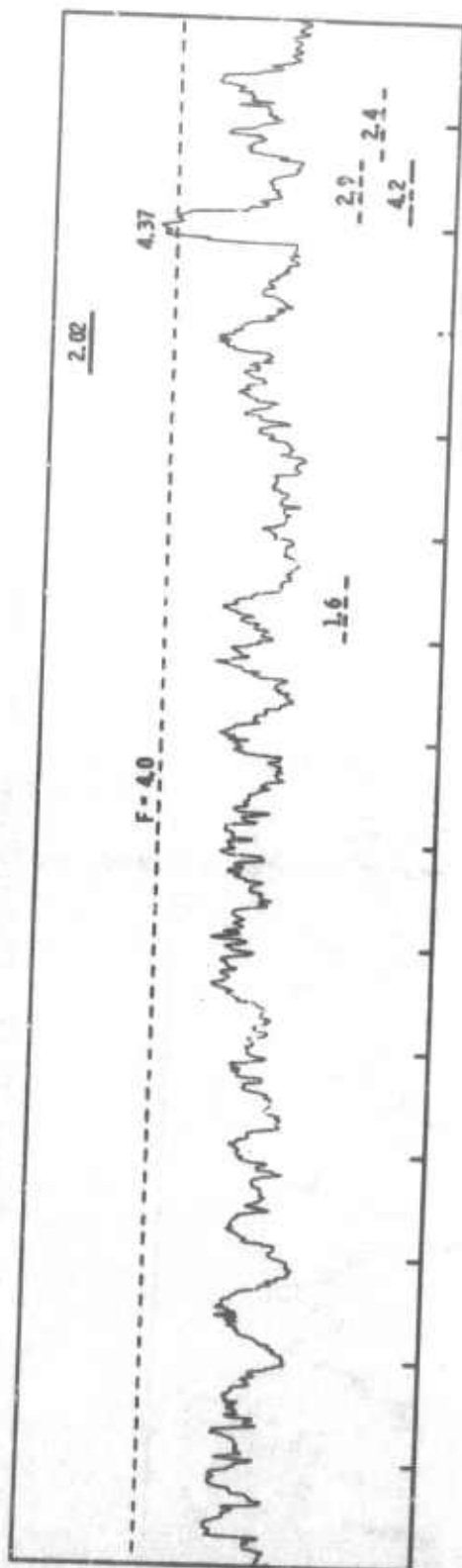Figure III-18. Fisher Time Traces for Filtered Traces of Subarray B3

——— 0.625 - 1.406 CPS BANDWIDTH
----- 1.25 - 2.031 CPS BANDWIDTH
----- 0.938 - 1.719 CPS BANDWIDTH
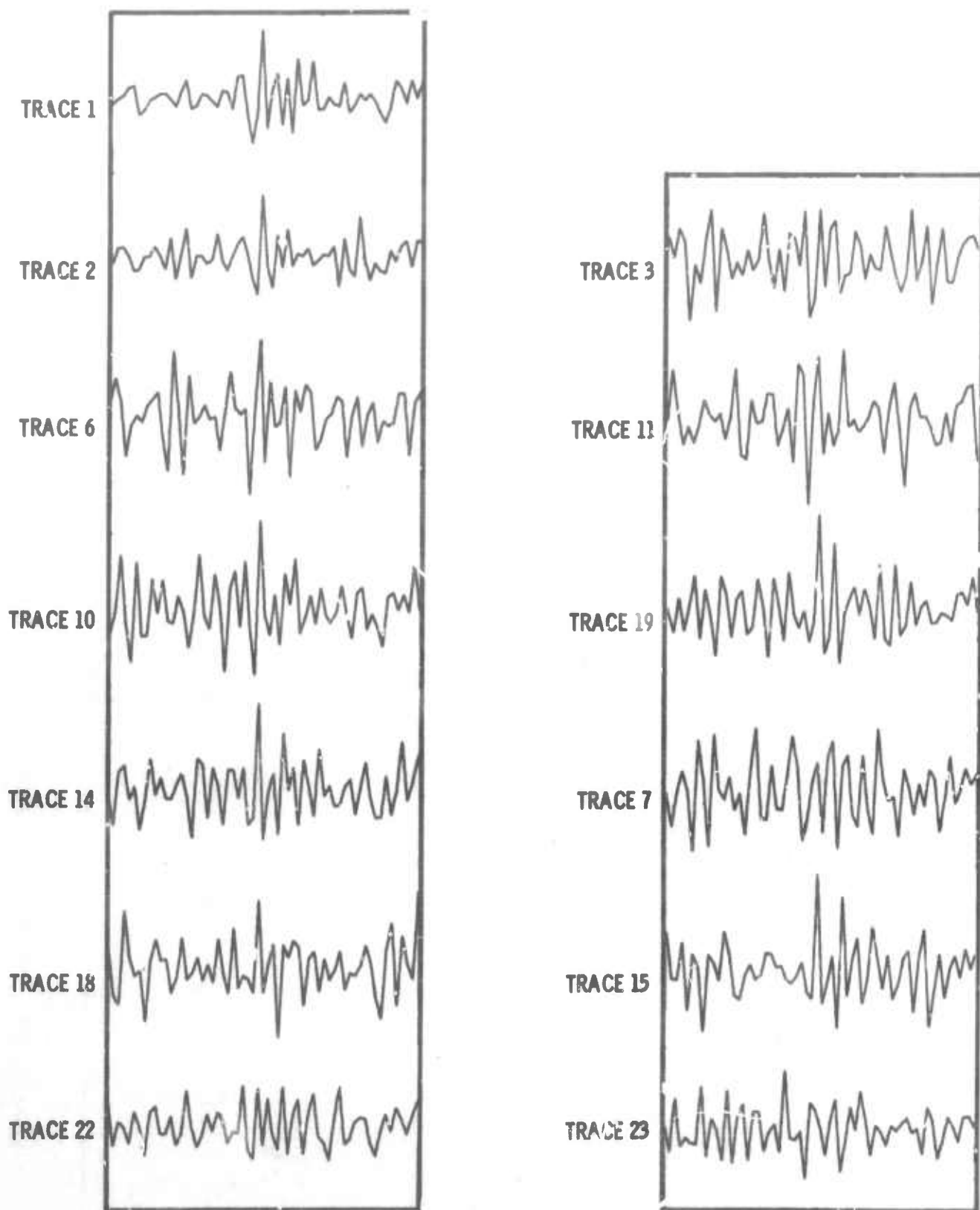
Figure III-19. Noise Segment Containing Signal Detected by Analysis-of-Variance Technique Applied to Subarray B3
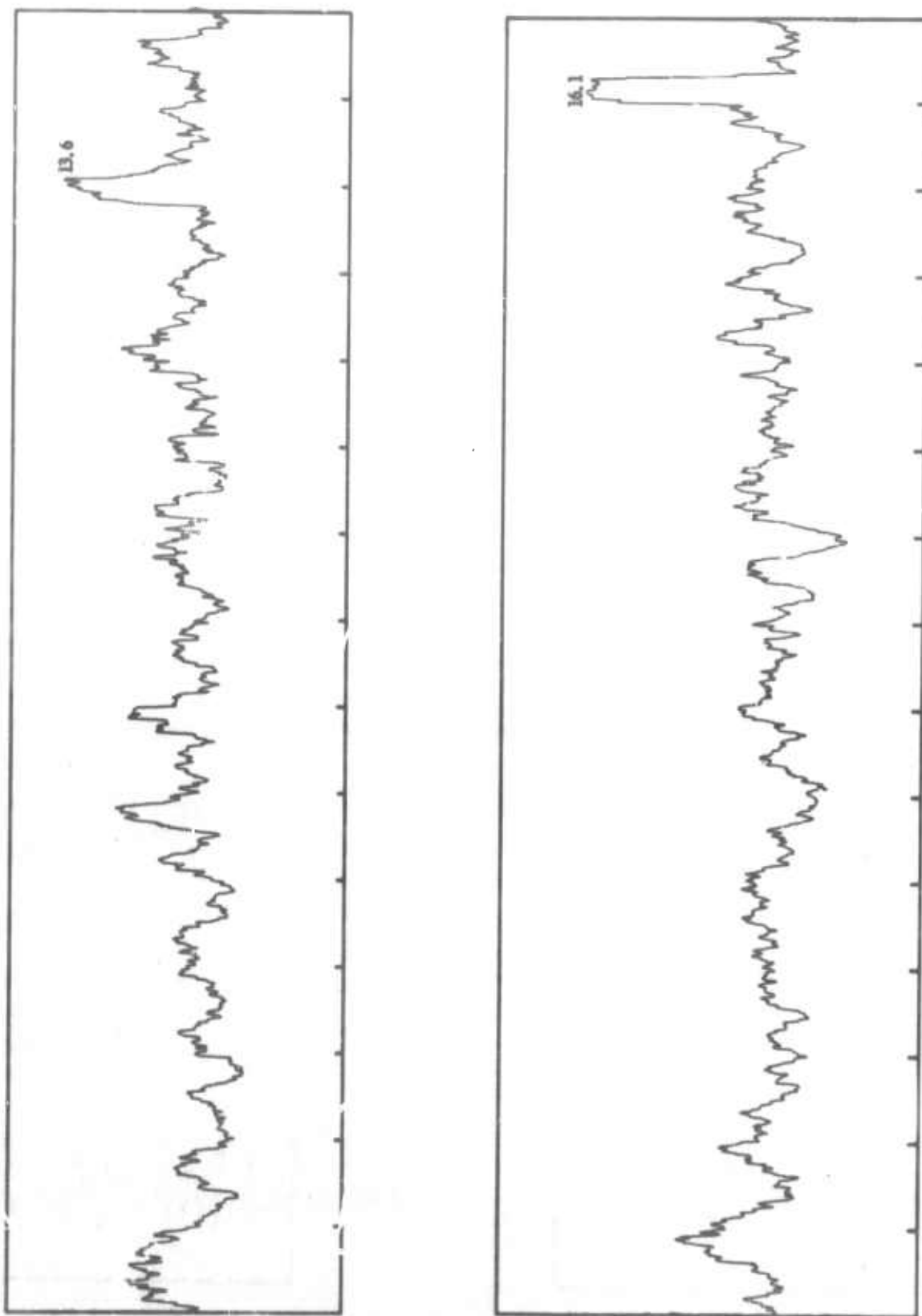
science services division

Figure III-20. Stacked Fisher Time Traces for Filtered Noise of Subarrays A0, B1, B2, B3

The maximum Fisher values of the first segment were 2.68, 4.74, 3.42, and 4.37 for subarrays A0, B1, B2, and B3, respectively. An inspection of the 13 filtered traces for each subarray in this area of the data revealed no visible signal. The second segment of noise had Fisher values of 2.3, 4.62, 2.3, and 9.09 for the four subarrays. A signal was visible in the filtered time traces of B1 and B3.

To determine the effect of wave velocity on the Fisher outputs, the four Fisher traces were time-shifted to correct for the moveout of a signal propagating with a velocity of 10 km/sec across the four subarrays from the north. Then, the resulting traces were summed. This procedure was repeated for signals traveling with the same velocity from the NW, SW, S, SE, and NE. Time corrections were also made for a signal propagating at 16 km/sec from the six directions. The resulting 12 traces had the same two predominant peaks as the sum of the Fisher output traces which had not been shifted (Figure III-20).

The dynamic-power-spectra technique was applied to the multichannel-filtered outputs of A0, B1, B2, and B3 in the three frequency bandwidths used in the embedded signal test case. The 64-point segments of noise which this method found to contain signals are indicated on the Fisher outputs in Figure III-15 through III-18. In each of these cases, most noise segments with vector magnitudes greater than 2.5 corresponded to peaks in the Fisher time traces. However, the noise segments in the Fisher outputs having the largest Fisher values did not have corresponding vectors of large magnitude; also, the dynamic-power-spectra method did not detect arrivals occurring at the same time within the four arrays.

In general, for both methods, there was a lack of correlation among the four subarrays of the noise segments found to contain possible discrete arrivals. In particular, neither technique indicated that an arrival was present in the segment of noise which was found to contain an arrival by the large-array analysis.

science services division

It appears unlikely that any highly coherent small P-wave
arrivals were present in the noise sample studied. A single discrete arrival
was indicated from the NE China area, but the "event" did not show up in the
subarray processing. This could have been masked by poorer S/N ratios for
the subarray processing. Within our ability to discriminate, therefore, it
appears that the P-wave noise does not contain a significant component com-
posed of discrete, coherent wavelets. Modeling of the P-wave noise as a
stationary Gaussian process appears to be most reasonable.

SECTION IV

REFERENCES

1. Richter, C.F., 1958: Elementary Seismology, W.H. Freeman and Co., San Francisco, Calif.

2. Texas Instruments Incorporated, 1962: Worldwide Collection and Evaluation of Earthquake Data, Semiannual Tech. Rpt. No. 3, Contract AF 19(604)8517, 31 Oct.

3. Teledyne Incorporated, 1965: Analysis of Variance as a Method of Signal Detection, Seismic Data Lab. Rpt. No. 116, Contract AF 33(657)12447, 25 Feb.

4. Cooley, J.W. and J.W. Tukey, 1965, An algorithm for the machine calculation of complex Fourier series: Mathematics of Computations, v. 19, Apr.

5. Haubrich, R.A., 1965: Earth noise, 5 to 500 millicycles per second: J. of Geophy. Res., v. 70, n. 6, 15 Mar.

6. Texas Instruments Incorporated, 1967: Space and Time Variability of LASA Noise Field, Large-Array Signal and Noise Analysis, Spec. Rpt. No. 4, Contract AF 33(657)-1678, (to be published).

7. Hildebrand, F.B., 1952: Introduction to Numerical Analysis, McGraw-Hill, p. 373-374.

8. Jenkins, G.M., 1961, General considerations in the analysis of spectra: Technometrics, v. 3, n. 2, May, p. 153.

science services division

APPENDIX A

DISTRIBUTION

APPENDIX A

χ^2 DISTRIBUTION

Consider a time trace $f(t)$ which has a normal distribution $[N(0, \sigma^2)]$. The Fourier transform yields

$$a_k = \sum_{n=0}^{N-1} f(t_n) \cos(2\pi kn/N) \quad k = 0, 1, \ldots, N-1$$

and

$$b_k = \sum_{n=0}^{N-1} f(t_n) \sin(2\pi kn/N)$$

If the $f(t_n)$ are independent, a_k is distributed as $N(0, A)$ where

$$A = \sigma^2 \sum_{n=0}^{N-1} \cos^2(2\pi kn/N) = \sigma^2 \left[N/2 + \sum_{n=0}^{N-1} \cos(4\pi kn/N) \right] = \sigma^2 \frac{N}{2}$$

for $k \neq 0$ or $N/2$ since

$$\sum_{n=0}^{N-1} \cos 4\pi kn/N = \text{real} \sum_{n=0}^{N-1} e^{\frac{4\pi kni}{N}} = \text{real} \left[\frac{e^{\frac{4\pi ki}{N}} - 1}{e^{\frac{4\pi ki}{N}} - 1} \right] = 0 + 0i$$

for $k \neq 0$ or $N/2$.

Similarly, b_k is distributed as $N(0, B)$ where

$$B = \sigma^2 \sum_{n=0}^{N-1} \sin^2(2\pi kn/N) = \sigma^2 \left[\frac{N}{2} - \sum_{n=0}^{N-1} \sin(4\pi kn/N) \right] = \sigma^2 \frac{N}{2}$$

for $k \neq 0$ or $N/2$.

Thus, $A = B$ and a_k and b_k are distributed as $N(0, \sigma'^2)$ and a_k/σ' and b_k/σ' are distributed as $N(0, 1)$. Squares of standard normal variables are distributed as χ^2 with one degree of freedom. Thus, $a_k^2/\sigma'^2 + b_k^2/\sigma'^2$ is distributed as χ_2^2 (two degrees of freedom), or $a_k^2 + b_k^2$ is distributed as $\sigma'^2 \chi_2^2$.

The independence of adjacent points in frequency is shown by

$$\text{cov}(a_j a_k) = E\left[\sum_{n=0}^{N-1} f(t_n) \cos(2\pi kn/N) \cdot \sum_{n=0}^{N-1} f(t_n) \sin(2\pi kn/N) \right]$$

for $j \neq k$. Using the independence of $f(t_n) f(t_m)$ with $m \neq n$ and since the cos and sin functions are orthogonal under this type of summation,[7] one has

$$\text{cov}(a_j a_k) = \sigma^2 \sum_{n=0}^{N-1} \cos(2\pi jn/N) \sin(2\pi kn/N) = 0$$

for $j \neq k$. These results are true asymptotically as N becomes large.[8]

APPENDIX B
DERIVATION OF FALSE-ALARM RATE

The functional form of χ_4^2 is

$$\frac{x}{4} \, e^{-x/2} \text{ for } x \geq 0 \text{ and } 0 \text{ for } x < 0$$

This has a mean of 4 and a variance of 8.

The frequencies calculated are independent (Appendix A). Thus, an n-dimensional frequency vector of the type used in this analysis would have components which are independent and distributed $a\chi_4^2$.

First, consider a 2-dimensional case which is easy to visualize; then, generalize from this case.

Given a vector $y = (x_1, x_2)$ where x_1 and x_2 are distributed $a\chi_4^2$ and independent, we wish to know the probability that $x_1 > N_1$, $x_2 > N_2$, and magnitude

$$\left[\left(\frac{X_1 - N_1}{\sigma_1} \right)^2 + \left(\frac{X_2 - N_2}{\sigma_2} \right)^2 \right]^{1/2} > R$$
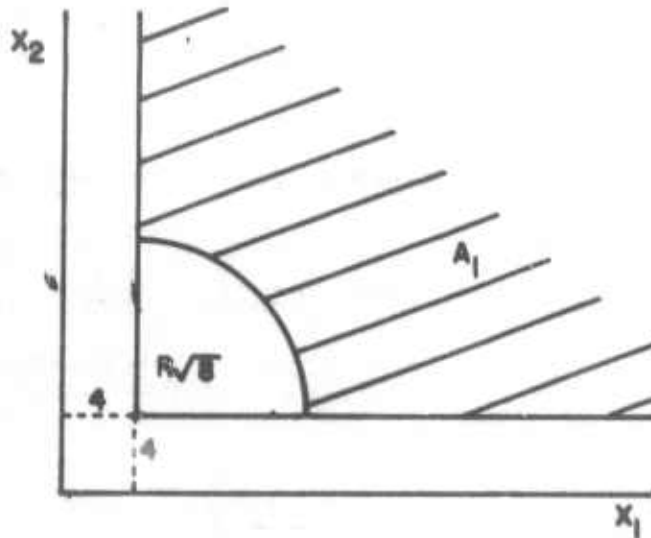
where

$$\sigma_1 = \sqrt{\sum_{\gamma=1}^{MB} \frac{(X_{i\gamma} - N_i)^2}{MB - 1}}$$

Assuming the estimates of the mean and the standard deviation to be correct, this is equivalent to wishing to know the probability, if given a vector $y = (x_1, x_2)$ where x_1 and x_2 are distributed χ_4^2 and independent, that $x_1 > 4$, $x_2 > 4$, and

$$\left[\left(\frac{x_1 - 4}{\sqrt{8}}\right)^2 + \left(\frac{x_2 - 4}{\sqrt{8}}\right)^2\right]^{1/2} > R$$

This is the integral of the joint distribution of $x_1 x_2$ over the shaded area shown below.

Since the components are independent, the joint distribution is the product of the individual distributions. One then has an integral of the form $\iint\limits_{A_1} \frac{x}{4} e^{-x/2} \; \frac{y}{4} e^{-y/2} \; dx \, dy$ to evaluate.

When the preceding is extended into three and four dimensions, the integral becomes quite complex. After a short attempt to get a closed-form expression for these integrals, the attempt was abandoned and a simplifying assumption made.

The circular sector (in two dimensions) is replaced by a square of equal area. To give an upper and lower bound, the circular sector is replaced by an inscribed square and a circumscribed square. (See figure below.)
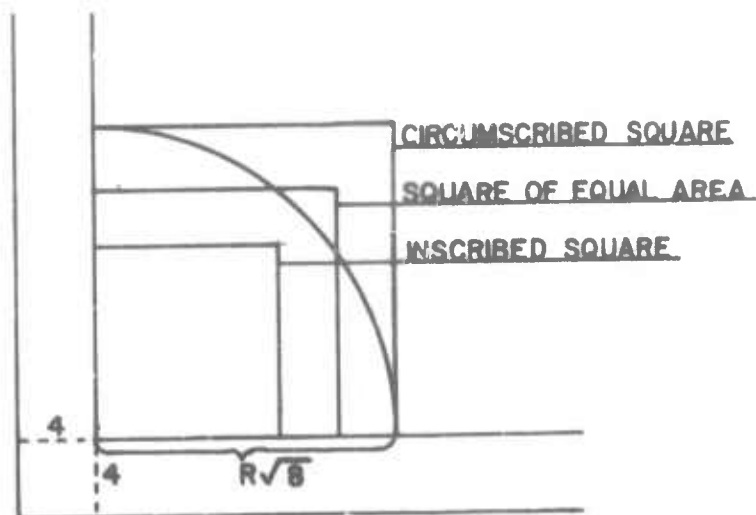
Extending this reasoning to higher dimensions, the probability integral for the 3-component (dimensional) case becomes

$$\left[\int_4^\infty \frac{x}{4} \, e^{-x/2} \, dx\right]^3 - \left[\int_4^a \frac{x}{4} \, e^{-x/2} \, dx\right]^3$$

and for the 4-component (dimensional) case,

$$\left[\int_4^\infty \frac{x}{4} \, e^{-x/2} \, dx\right]^4 - \left[\int_4^a \frac{x}{4} \, e^{-x/2} \, dx\right]^4$$

where a is the length of a side of the cube or hypercube.

These integrals were evaluated as a function of R. The results are shown in Figures II-1 and II-2.

Experience with generated Gaussian noise suggests that the equal "volume" curves give good agreement with experimental results.

DOCUMENT CONTROL DATA - R&D

(Security classification of title, body of abstract and indexing annotation must be entered when the overall report is classified)

1. ORIGINATING ACTIVITY (Corporate author)	2a. REPORT SECURITY CLASSIFICATION
Texas Instruments Incorporated Science Services Division P.O. Box 5621, Dallas, Texas 75222	Unclassified
	2b. GROUP

3. REPORT TITLE

DETECTION OF DISCRETE ARRIVALS IN MANTLE P-WAVE NOISE
LARGE-ARRAY SIGNAL AND NOISE ANALYSIS — SPECIAL SCIENTIFIC
REPORT NO. 5

4. DESCRIPTIVE NOTES (Type of report and inclusive dates)

Special

5. AUTHOR(S) (Last name, first name, initial)

Crouch, Donald B.

6. REPORT DATE	7a. TOTAL NO. OF PAGES	7b. NO. OF REFS
6 September 1967	55	8

8a. CONTRACT OR GRANT NO.	9a. ORIGINATOR'S REPORT NUMBER(S)
Contract No. AF 33(657)-16678	
b. PROJECT NO. AFTAC Project No. VT/6707	
c.	9b. OTHER REPORT NO(S) (Any other numbers that may be assigned this report)
d	

10. AVAILABILITY/LIMITATION NOTICES

This document is subject to special export controls and each transmittal to
foreign governments or foreign nationals may be made only with prior
approval of Chief, AFTAC.

11. SUPPLEMENTARY NOTES	12. SPONSORING MILITARY ACTIVITY
ARPA Order No. 599	Air Force Technical Applications Center VELA Seismological Center Headquarters, USAF, Washington, D.C.

13. ABSTRACT

An exponential relation, $\log N = a - bM$ where N is the annual number of
earthquakes of magnitude M, is generally accepted to exist between the number
of earthquakes occurring in a given time and the earthquake magnitude. A
linear least-squares solution of this equation indicates that a small earthquake
($2 < M < 3$) occurs every 30 sec. The only difference between these small
P waves and an event is one of magnitude; therefore, it is reasonable to expect
that the P-wave noise would contain discrete P-wave arrivals which travel
across the array as plane waves. The purpose of this study is to identify and
describe (statistically) such discrete arrivals.

Two techniques have been used to identify discrete arrivals. One method,
Fisher analysis of variance, provides an output time function which measures
the likelihood of an arrival in a specific segment of noise. The other technique
calculates a moving power spectra and looks for spectral characteristics
which are sufficiently deviant from the expected values of a Gaussian stationary
process. Using an 8-min noise sample, the methods were able to detect no
discrete arrivals propagating across the array as plane waves. Within the
resolving power of these tests, no small P wavelets appeared to be in the
mantle P-wave noise.

DD FORM 1473 (1 JAN 64)

14 KEY WORDS	LINK A		LINK B		LINK C	
	ROLE	WT	ROLE	WT	ROLE	WT
Large-Array Signal and Noise Analysis						
Detection of Discrete Arrivals						
Fisher Analysis of Varince						
Moving Power Spectra						

INSTRUCTIONS

1. ORIGINATING ACTIVITY: Enter the name end address of the contractor, subcontractor, grantee, Department of Defense activity or other organization (corporate author) issuing the report.

2a. REPORT SECURITY CLASSIFICATION: Enter the overell security classification of the report. Indicate whether "Restricted Data" is included. Marking is to be in accordence with appropriate security regulations.

2b. GROUP: Automatic downgrading is specified in DoD Directive 5200.10 and Armed Forces Industriel Menual. Enter the group number. Also, when eppliceble, show that optional merkings have been used for Group 3 end Group 4 ea euthorized.

3. REPORT TITLE: Enter the complete report title in all cepital letters. Titlea in all cases should be unclassified. If e meeningful title cannot be aelected without clessification, show title classification in ail cepitels in parenthesia immediately following the title.

4. DESCRIPTIVE NOTES: If appropriate, enter the type of report, e.g., interim, progress, summary, annual, or final. Give the incluaive dates when a specific reporting period is covered.

5. AUTHOR(S): Enter the name(s) of euthor(s) aa shown on or in the report. Enter last neme, first name, middle initial. If military, show renk end branch of service. The name of the principal author is an absolute minimum requirement.

6. REPORT DATE: Enter the data of the report ea day, month, year; or month, year. If more then one date appeara on the report, uae dete of publication.

7a. TOTAL NUMBER OF PAGES: The total page count should follow normal pagination procedures, i.e., enter the number of pages containing information.

7b. NUMBER OF REFERENCES: Enter the total number of references cited in the report.

8a. CONTRACT OR GRANT NUMBER: If appropriate, enter the applicable number of the contract or grant under which the report was written.

8b, 8c, & 8d. PROJECT NUMBER: Enter the appropriate military department identification, such aa project number, aubproject number, ayatem numbera, taak number, etc.

9a. ORIGINATOR'S REPORT NUMBER(S): Enter the official report number by which the document will be identified and controlled by the originating activity. This number must be unique to this report.

9b. OTHER REPORT NUMBER(S): If the report has been assigned any oiher report numbera (either by the originator or by the eponeor), also enter this number(a).

10. AVAILABILITY/LIMITATION NOTICES: Enter any limitationa on further diasemination of the report, other than those imposed by security classification, using standard stetements such ae:

(1) "Qualified requesters may obtain copies of this report from DDC."

(2) "Foreign announcement end diasemination of this report by DDC is not authorized."

(3) "U. S. Government egencies mey obtain copies of this report directly from DDC. Other qualified DDC users ahell request through
_____."

(4) "U. S. military egencies may obtein copies of this report directly from DDC. Other quelified users shell request through
_____."

(5) "All diatribution of this report is controlled. Qualified DDC users shell request through
_____."

If the report has been furnished to the Office of Technicel Services, Department of Commerce, for sele to the public, indicete this fact and enter the price, if known.

11. SUPPLEMENTARY NOTES: Use for additional explanatory notes.

12. SPONSORING MILITARY ACTIVITY: Enter the name of the departmentel project office or laboratory sponsoring (peying for) the research and development. Include eddress.

13. ABSTRACT: Enter en ebstract giving e brief and fectual summery of the document indicative of the report, even though it may also appear elsewhere in the body of the technical report. If edditional space is required, e continuetion sheet shell be ettached.

It is highly desirable that the ebstract of classified reporta be unclassified. Each paragraph of the ebstract shell end with an indicetion of the military aecurity clessificetion of the information in the paragraph, represented ea (TS) (S), (C), or (U).

There ia no limitation on the length of the ebstract. However, the auggeated length is from 150 to 225 words.

14. KEY WORDS: Key words are technically meeningful terma or short phreaes that cheracterize a repor, and may be used ea index entries for cataloging the report. Key words must be aelected ao that no security clessificetion is required. Identifiers, such aa equipment model deaignetion, trade name, military project code name, geographic location, may be used as key words but will be followed by en indicetion of technicel context. The assignment of links, rules, and weights ia optionel.